Trichoderma afroharzianum T22 induces rhizobia and flavonoid through systemic signaling to combat Fe deficiency in garden pea

Asha Thapa, Md Rokibul Hasan, Ahmad H. Kabir*
School of Sciences, University of Louisiana at Monroe, Monroe, LA 71209, USA
*e-mail: kabir@ulm.edu

ABSTRACT

Iron (Fe) deficiency is a limiting factor for garden peas, yet the role of beneficial fungi in addressing this issue is understudied. In this study, *Trichoderma afroharzianum* T22 colonized the roots of Fe-deficient pea cultivars in Cultivar-dependent manner. In Sugar Snap, T22 improved growth parameters consistent with increased tissue Fe and rhizosphere siderophore under Fe deficiency. RNA-seq analysis showed 575 and 818 differentially expressed genes upregulated and downregulated in roots of Fe-deficient pea inoculated with T22. The upregulated genes (monooxygenase activity, ammonia-lyase activity, 4-coumarate-CoA ligase) are involved in flavonoid biosynthesis, along with genes related to mineral transport and redox homeostasis. Further, split-root assay demonstrated systemic signaling between T22 and the host promoting symbiotic associations. Interestingly, T22 restored the abundance of rhizobia, particularly *Rhizobium leguminosarum* and *Rhizobium indicum*, along with the induction of *NifA*, *NifD*, and *NifH* in nodules, suggesting a connection between T22 and rhizobia in Fe-starved peas. A flavonoid precursor restored plant health even in the absence of T22, possibly promoting microbial symbiosis in mitigating Fe deficiency. Further, the elevated siderophore and root flavonoid diminished when T22 was substituted with Fe, eliminating the need for microbiome-driven Fe mobilization which was further supported by the positive interaction of T22 on *R. leguminosarum* growth in Fe-deficient media. Thus, the beneficial effect of T22 on rhizobia likely stems from their interactions, not just improved Fe status in plants. This study provides the first mechanistic insights into T22 interactions with host and rhizobia, advancing microbiome strategies to alleviate Fe deficiency in peas and other legumes.

Keywords: Abiotic stress, chlorosis, legume crop, biostimulant, siderophore, symbiosis.

Running title: Fe deficiency mitigation in pea with T22

1. INTRODUCTION

Fe (Fe) is an abundant element on earth and is a biologically essential component of every living organism, including plants (Connorton et al. 2017). However, several soil factors can affect the availability of Fe to plants. These include, but are not limited to, high soil pH due to elevated bicarbonate and salt, soil with a high cation exchange capacity, high levels of oxides, and low organic matter in the soil (Zhao et al. 2020; Alcántara et al. 2000; Kroh and Pilon 2019). Fe deficiency in soil may lead to reduced Fe accumulation in crops resulting in leaf chlorosis, photosynthetic disturbance, stunted growth, reduced root growth, redox imbalance, and poor yield in crops (Kabir et al. 2022; Sun et al. 2016). Specifically, this deficiency in legume crops can be severe, primarily because of the high levels of Fe required for nodule formation (Brear et al. 2013). Fe deficiency can influence both the legume host and the rhizobia individually, or it can directly affect their interaction (Brear et al. 2013; Dixon and Kahn 2004). It has been observed that *Rhizobium leguminosarum* is a prevalent type of rhizobia capable of forming nitrogen-fixing nodules on pea roots (Boeglin et al. 2022).

Different plants have different strategies for Fe uptake. Dicot plants consist of a set of mechanisms known as strategy I plants (Waters et al. 2018; Curie and Briat 2003). Plants employing strategy I typically possess ferric chelate reductase activity, converting Fe(III) to readily available Fe(II) for plants (Kabir et al. 2012). The acidification of the rhizosphere via H^+ secretion is another important method plants utilize to solubilize soil Fe (Molnár et al. 2023; Kabir et al. 2012). In addition, phenolic compounds, released through root exudates, exhibit chelating and reducing actions in response to Fe shortage in plants (Curie and Mari 2017; Rodríguez-Celma and Schmidt 2013). Following that, the uptake of solubilized Fe into the root system is facilitated by metal transporters, *IRT1* (Fe-regulated transporter), commonly found in several plant species (Kabir et al. 2012; Vert et al. 2001). However, the induction of strategy I responses largely depends on the genetic factors of the cultivar, which can render many popular and high-yielding genetic lines of crops, sensitive to Fe deficiency.

Plants can accommodate a vast array of microorganisms in and around their organs which may offer a sustainable solution for fortifying crops with the supply of Fe. Among the beneficial fungi, arbuscular mycorrhizal fungi (AMF) appear to be almost exclusively studied for their helpful role in plants. However, *Trichoderma* spp. is one of the main groups of rhizosphere mycorrhizal fungi, other than AMF, that can promote plant growth and development through a variety of means (Harman et al. 2004; Qi and Zhao 2013). Of them, *T. afroharzianum* T22 has already demonstrated shreds of evidence for plant growth promotion and stress tolerance (Bjørk et al. 2023; Kabir et al. 2022). However, there are undoubtedly still a lot of unanswered questions regarding the mechanisms of connection of this fungus with host plants in response to abiotic stresses. In a previous study, we reported that T22 triggered Strategy-I responses in Fe-deficient soybean, leading to the upregulation of *GmFRO2* and *GmIRT1* (Kabir et al. 2022). Recent research has shown that T22 significantly upregulated multiple genes related to Fe uptake, auxin synthesis, nicotianamine synthase 3, and phytosiderophore transporter 1, aiding sorghum plants in coping with Fe deficiency (Kabir and Bennetzen 2024). Studies suggest that fungi-plant symbiosis is involved in local and/or systemic signaling, predominantly depending on host genetic factors (Giovannetti et al. 2024; MacLean et al. 2017). Symbiosis requires continual signaling between

the symbionts and the activation of new transcriptional programs in the plant host, especially in the roots (Bucher et al. 2014). This process triggers changes essential for the plant cell to host the fungal endosymbiont and maintain symbiosis. Of many molecules involved in symbiosis, phytohormones play a key role in the symbiosis between most land plants and fungi (Liao et al. 2018; Lopez-Obando et al. 2015). Other than plant hormones, flavonoids released by plants, have been found to promote microbial colonization and serve as pre-symbiotic signaling molecules in microbial-plant symbiosis (Lidoy et al. 2023; Schliemann et al. 2008). Coumarins, secondary metabolites synthesized via the phenylpropanoid pathway in plants, act as signaling molecules regulating interactions between symbiotic microbes and plants (Harbort et al. 2020; Stringlis et al. 2009). However, this information is still limited to very few crops.

Garden pea (*Pisum sativum* ssp. hortense) holds significant relevance as a pulse as well as a research crop due to its nutritional value, genetic diversity, and genetic tools (Pandey et al. 2022; Hacisalihoglu et al. 2021; Chaudhari et al. 2020). To address Fe deficiency in crops, growers typically use soil amendments and fertilizers that are not only costly but also environmentally unsafe. There are pieces of evidence of the microbiome's positive role in enhancing Fe status in plants (Kabir and Bennetzen 2024; Kabir et al. 2022; Bhardwaj et al. 2014). However, the specific role and mechanistic basis of T22 in pea plants and its nodule formation under Fe deficiency, remain unclear. Therefore, we investigated whether the colonization of T22 occurs in a host-specific manner and how it influences transcriptional changes in host plants, inducing symbiotic signaling and tolerance to Fe deficiency in garden pea. We further elucidated whether the restoration of rhizobia abundance in root nodules is attributed to the direct impact of T22 on rhizobia or the indirect influence of T22 on improving Fe availability in Fe-deficient peas.

2. MATERIALS AND METHODS

2.1 Plant cultivation and growth conditions

The seeds of six cultivars of garden peas (Lillian, Little Marvel, Green Arrow, Sugar Sprint, Sugar Bon, and Sugar Snap) were used in this study. After the initial screening, Sugar Snap was used for the rest of the experiments. Briefly, the seeds were surface sterilized with a 4% sodium hypochlorite solution for 5 min, washed three times with sterile water, and finally placed in a tray in an incubator at 25°C for 2 d. After germination, uniform and healthy seedlings were cultivated in a soil pot (500 g soil) containing natural field soil and commercial potting mix (1:2) in four different treatments of lime ($NaHCO_3$ and g $CaCO_3$) and *Trichoderma afroharzianum* T22 as follows: (i) control (soil without lime pH ~6.0), (ii) Fe- (soil mixed with lime pH ~7.8), (iii) Fe-T22+ (soil mixed with lime pH ~7.8 and T22 *inoculum* (1×10^9 cfu/gram) and (iv) T22+ (soil without lime pH ~6.0 and T22 *inoculum* (1×10^9 cfu/gram). Also, the T22 inoculum was cultured on potato dextrose agar (PDA) medium to verify the viability of the fungal spores before inoculation (Supplementary Fig. S1). During the cultivation period, we added 15 mM $NaHCO_3$ weekly to maintain the pH of the Fe-deficient soil to 7.8 which caused indirect Fe deficiency in plants. This cultivation was conducted up to 4-week before data measurement.

In a targeted experiment, cinnamic acid, a precursor of the flavonoid synthesis pathway (Li et al. 2020), was supplemented in soil (0.5/500 g soil) to study whether it can induce Fe deficiency tolerance in plants in the absence of exogenous T22. In another study, we added two additional treatment groups as follows: Fe- FeEDDHA+ (soil mixed with lime, pH ~7.8, and FeEDDHA at a dose of 0.5/500 g soil) and control (soil without lime, pH ~6.0, and Fe-EDDTA at a dose of 0.5/500 g soil). These two targeted studies were conducted for 5 weeks before data analysis. In all

cultivations, plants were grown in a randomized complete block design with 9 biological replications per treatment in a growth chamber with 10 h of light and 14 h of darkness (250 µmol m^{-2} s^{-1}) at ~25°C. Also, the physicochemical characteristics of the soil are detailed in Supplementary Table S1.

2.2 Measurement of morphological features and chlorophyll fluorescence kinetics

The shoot height and root length of each plant were measured using a measuring tape. Subsequently, the harvested shoot and root were dried for 3 d at 70°C in an electric oven before recording their dry weight. For nodule calculation, the roots were gently washed to remove soil particles. Nodules were then carefully harvested from the root system, counted using a magnifying lens, and stored in an 80°C freezer for further analysis. In addition, chlorophyll score and chlorophyll fluorescence kinetics (OJIP), such as Fv/Fm (maximal photochemical efficiency of PSII and Pi-ABS (photosynthesis performance index), were measured on the uppermost fully developed leaves on three different spots using a handheld chlorophyll meter (AMTAST, United States) and FluorPen FP 110 (Photon Systems Instruments, Czech Republic), respectively. For OJIP analysis, the leaves were adapted to dark for 1 h before data measurement.

2.3 Molecular detection of T22 colonization in roots

Considering the potential variation of T22 colonization across different root sections of garden pea, we performed root partitions to identify a representative part with the most abundant colonization. Briefly, we divided the roots into four segments: the mature zone (1–3 cm), elongation zone (3–6 cm), meristematic zone (6 cm and beyond), and root tips, as illustrated in Supplementary Fig. S3. The establishment and colonization of T22 in roots of Sugar Snap cultivated under Fe deficiency were assessed by DNA-based qPCR (Kabir and Bennetzen, 2024). Briefly, root samples were washed twice in fresh sterile phosphate-buffered saline, followed by a brief vortex and two rinses with sterile water. The DNA was extracted on approximately 0.2 g of root samples using CTAB (cetyl trimethylammonium bromide) method (Clarke, 2009). Subsequently, DNA was quantified using a NanoDrop ND-1000 Spectrophotometer (Wilmington, USA) and diluted to equal quantities for each DNA sample. The qPCR analysis was conducted using a CFX96 Touch Real-Time PCR Detection System (Bio-Rad, USA), with specific primers (forward: 5′-GTC GGT AGC TGA AAG GGG AT-3′; reverse: 5′-AT TAG AGG CCG GAA ACA CC-3′) designed to amplify a fragment of *TaAOX1* (L-aminoacid oxidase gene) of T22 (Kabir and Bennetzen 2024). The iTaq™ Universal SYBR® Green Supermix (Bio-Rad, USA) was used in all reactions along with gene-specific primers (Supplementary Table S2) for *PsGAPDH* that served as the internal control for relative quantification using $2^{-\Delta\Delta}$CT method (Livak and Schmittgen, 2001).

2.4 Determinations of siderophore levels in the rhizosphere

We determined the siderophore content in rhizosphere soil using a chrome azurol S (CAS) assay (Himpsl and Mobley 2019). In brief, rhizosphere soil was homogenized with 80% methanol and centrifuged for 15 min at 10,000 rpm. The resulting supernatant (500 µl) was combined with 500 µl of CAS solution and incubated at room temperature for 5 min. Absorbance was then measured at 630 nm using 1 ml of CAS reagent as a reference. Siderophore levels per gram of soil sample were calculated with the formula: % siderophore unit = [(Ar - As) / Ar] x 100, where Ar is the absorbance of the reference (CAS reagent only) at 630 nm and As is the absorbance of the sample (CAS reagent + soil sample) at 630 nm.

186 **2.5 Nutrient analysis in root and shoot**
187 Nutrient analysis was performed on both roots and young leaves. The roots were cut, washed with
188 running tap water, and then immersed in 0.1 mM $CaSO_4$ for 10 min, followed by a rinse with
189 deionized water. Young leaves were separately washed with deionized water. All samples were
190 placed in individual envelopes and dried in an electric oven at 75°C for 3 days. Elemental
191 concentrations were measured using inductively coupled plasma mass spectrometry (ICP-MS) at
192 the Agricultural and Environment Services Laboratories at the University of Georgia.
193
194 **2.6 Split-root assay**
195 The plants were cultivated for 2 weeks in sterile vermiculite before performing the split root assay.
196 This was done using a single pot/chamber with a partitioned split-root assembly with some
197 modifications as previously described (Thilakarathna and Cope 2021). Then, the taproot of each
198 seedling was cut in the middle with scissors, and the lateral root system was evenly divided into
199 two compartments filled with natural field soil and commercial potting mix (1:2) as described
200 earlier. The two compartments were separated by a solid plastic barrier. The plant growth
201 conditions (presence or absence of Fe deficiency) were the same, except that one compartment of
202 each split-root system was inoculated with T22 while the other was not, depending on the treatment
203 type. The split-root plants were cultivated for another four weeks before data measurement. The
204 split-root cultivation was performed in three different conditions: control/control (-/-), T22/T22
205 (+/+), and control/T22 (-/+). Data was collected after 4 weeks of cultivation in a split-root system.
206
207 **2.7 RNA-sequencing and bioinformatics analysis**
208 RNA-seq analysis was performed on roots collected from the meristematic zone. Before RNA
209 extraction, the roots were cleaned by rinsing them twice with sterile water after being vortexed
210 twice for 10 sec in sterile phosphate-buffered saline to get rid of any surface contaminants. The
211 samples were ground into a powder using liquid nitrogen and a pre-cooled pestle and mortar for
212 RNA extraction in accordance with the SV Total RNA Isolation System (Promega Corporation,
213 USA). One microgram of RNA (per sample) with a RIN value higher than 8 was used as the input
214 material for RNA-seq library preparations. Sequencing libraries were generated using the
215 TapeStation HS D1000 Kit (Agilent Technologies, USA), following the manufacturer's
216 instructions. The libraries were sequenced on an Illumina NovaSeq 6000 instrument using 0.2
217 Shared S4 150 bp paired-end sequencing at RTSF Genomics Core at Michigan State University.
218 Overall, 92.5% of reads passed filters with a quality score of ≥ Q30, yielding 917.23 Gbp of data.
219
220 Bioinformatics analysis of raw FastQ files was performed using Partek Flow genomic analysis
221 software (Partek, St. Louis, MO, USA). High-quality clean reads were obtained, by eliminating
222 adaptor sequences and low-quality sequences, from the raw reads with the Trimmomatic tool
223 (Bolger et al.2014). The clean reads were aligned to pea reference genome using HISAT2 (Kim et
224 al.2015). Read counts mapped to each gene were quantified using HTSeq (Anders et al.2015).
225 Differentially expressed genes (DEGs), which exhibited an adjusted P-value of < 0.05 and a fold
226 change of 2 or greater, were identified using the false discovery rate (FDR) method implemented
227 in the DESeq2 R package (v1.16.1), calculated based on FPKM (fragments per kilobase of exon
228 per million mapped fragments). Venn diagrams were generated using VennDetail (Hinder et al.
229 2017), and heatmaps were constructed using pheatmap (Hu et al. 2021) in the R programming
230 environment. The gene enrichment analyses of garden pea DEGs were performed using ShinyGO

0.76.3 (Ge et al. 2020), with gene ontology data retrieved from EnsemblPlants resources (Yates et al. 2022).

2.8 Nanopore-based 16S sequencing in root nodules

Isolated nodules were washed with running tap water, then surface-sterilized in a 3% sodium hypochlorite solution for 3 min and rinsed three times with sterilized distilled water. Total DNA was extracted using the CTAB method as previously described (Clarke 2009). PCR reactions were conducted using 5 ng of DNA from each sample and 16S primers 27F (AGAGTTTGATCMTGGCTCAG) and 1492R (CGGTTACCTTGTTACGACTT) to amplify the near full-length bacterial 16S rRNA gene. Thermal cycling conditions for PCR included an initial denaturation at 95°C for 2 min, followed by 30 cycles of denaturation at 95°C for 30 sec, annealing at 60°C for 30 sec, and extension at 72°C for 2 min. This was followed by a final extension at 72°C for 10 min and a hold at 4°C. Amplicons from each sample were ligated to pooled barcoded reads using the 16S Barcoding Kit 24 V14 (SQK-16S114.24, Oxford Nanopore Technologies, Oxford, UK) for library construction. Sequencing was carried out on MinION portable sequencer (Oxford Nanopore Technologies) using a Flongle flow cell (R10.4.1). The MinION™ sequencing data (FASTQ files) were processed using the EPI2ME software from Oxford Nanopore Technologies to produce pass reads with an average quality score > 9. The EPI2ME Fastq Barcoding workflow (Oxford Nanopore Technologies) was used for trimming adapter and barcode sequences. Principal coordination analysis, alpha diversity, and relative abundance of the bacterial community were calculated by R package phyloseq and vegan. Non-parametric Kruskal–Wallis tests were used to identify differences in taxa abundance at a 5% significance level (McMurdie and Holmes, 2013).

2.9 Real-time qPCR analysis of nitrogen-fixing genes in root nodules

Before RNA extraction from pea nodules, surface contaminants were thoroughly removed by washing with PBS buffer. RNA extraction and cDNA conversion were performed using the SV Total RNA Isolation System (Promega Corporation, USA) and GoScript™ Reverse Transcriptase (Promega Corporation, USA) kits, respectively. Subsequently, the expressions of *NifA* (nitrogenase Fe protein regulatory protein), *NifD* (nitrogenase FeMo protein alpha subunit), and *NifH* (nitrogenase FeMo protein beta subunit) associated with the nitrogen fixation process in diazotrophic bacteria were studied using gene-specific primers (Supplementary Table S3) in CFX96 Real-Time system (Bio-Rad, USA). The qPCR reaction was conducted with an initial denaturation at 95°C for 3 min, followed by 40 cycles of denaturation at 95°C for 5 sec, annealing at 55°C for 30 sec, and extension at 60°C for 5 min. Expression levels of target genes were analyzed using the $dd^{-\Delta Ct}$ method (Livak and Schmittgen, 2001), with normalization to *PsGAPDH*.

2.10 Determination of total flavonoid in roots

The total flavonoid content was measured in pea roots as previously described (Piyanete et al. 2009). Briefly, 0.5 mL of a 70% ethanol extract from the roots was mixed with 2 mL of distilled water and 0.15 mL of a 5% $NaNO_2$ solution. After incubating for 6 min, 0.15 mL of a 10% $AlCl_3$ solution was added, and the mixture was left to stand for another 6 min. Then, 2 mL of a 4% NaOH solution was added. The mixture was diluted to a final volume of 5 mL with methanol and thoroughly mixed. After a 15-min incubation period, the absorbance was measured at 510 nm using a spectrophotometer against a blank. The total flavonoid concentration was expressed in milligrams per gram of dry weight, calculated using a quercetin standard curve.

2.11 Microbial co-culture method

We studied the interactions between T22 and *R. leguminosarum* under *in vitro* nutrient agar conditions in both Fe-sufficient and Fe-deficient supplemented with 15 mM $NaHCO_3$ to increase the pH to 7.8. The microbial species (5 µl inoculum) were cultured in three different combinations: T22 alone, *R. leguminosarum* alone, and T22 + *R. leguminosarum*. The growth of the microbial species was measured after 7 days of culture using ImageJ software (National Institutes of Health, USA). The radius of microbial colonies was measured at three points and then averaged.

2.12 Data analysis

The statistical significance of each variable was assessed through analysis of variance (ANOVA), with the treatment considered as the independent variable. Subsequently, Duncan's Multiple Range post-hoc test (DMRT) was conducted using SPSS Statistics 20.0 (IBM). Graphical presentations were prepared using GraphPad Prism 7 and the R (ggplot2) program.

3. RESULTS

3.1 Effect of T22 on root colonization and morphological features

The colonization efficiency of T22 in roots and its effect on growth parameters of different Cultivars of garden peas exposed to Fe deficiency was evaluated. The relative abundance of *TaAOX1* showed a substantial variation in roots across different plant cultivars and treatment groups (Supplementary Fig. S1A). In general, the relative abundance of *TaAOX1* showed no significant differences in the roots of Lillian, Little Marvel, Green Arrow, and Sugar Sprint either inoculated with T22 or not in the presence or absence of Fe deficiency in the soil. In Sugar Bon and Sugar Snap, Fe deficiency caused no significant changes in the relative abundance of *TaAOX1*. However, Fe-deficient plants inoculated with T22 showed a significant increase in *TaAOX1* relative to Fe-starved plants in these two cultivars. Under Fe-sufficient conditions, T22 inoculation increased *TaAOX1* expression in Sugar Bon but decreased it in Sugar Snap compared to Fe-TA+ conditions (Supplementary Fig. S1A).

Lillian showed no significant changes in chlorophyll score in response to Fe deficiency compared to controls (Supplementary Fig. S1B). Interestingly, Fe-deficient plants inoculated with T22 caused a significant decline in chlorophyll score relative to Fe-deficient and control plants. Plants inoculated with T22 with Fe sufficient still showed a significant decrease in chlorophyll score compared to plants either with Fe sufficiency or Fe deficiency but not inoculated with T22 (Supplementary Fig. S1B). Although the chlorophyll score was significantly decreased due to Fe deficiency relative to controls, the addition of T22 with Fe deficiency caused no significant changes in the chlorophyll score of Little Marvel (Supplementary Fig. S1B). Green Arrow and Sugar Sprint showed no significant alternations in chlorophyll score regardless of the Fe availability in the presence or absence of T22 (Supplementary Fig. S1B). Furthermore, Sugar Bon and Sugar Snap showed a significant reduction in chlorophyll scores under Fe-deficient conditions; however, chlorophyll scores increased significantly in Sugar Snap but not in Sugar Bon when Fe-deficient plants were supplemented with T22. Fe-sufficient plants inoculated with T22 showed a similar chlorophyll score to Fe-sufficient controls in these two cultivars (Supplementary Fig. S1B).

Under Fe-deficient conditions, there was a significant decrease in root length and root dry weight for Lillian and Little Marvel (Supplementary Fig. S1C-S1D). However, T22 did not improve root length or root dry weight in these cultivars under Fe-deficient conditions (Supplementary Fig.

S1C-S1D). In Green Arrow, root length and root dry weight significantly decreased under Fe deficiency but increased under Fe-sufficient conditions when inoculated with T22 in both scenarios (Supplementary Fig. S1C-S1D). In this study, Sugar Sprint and Sugar Bon showed no significant differences in root length between Fe-sufficient and Fe-deficient conditions (Supplementary Fig. S1C). However, root dry weight in Sugar Bon was significantly reduced under Fe-deficiency compared to controls. However, T22 inoculated under Fe deficiency showed no significant changes in root dry weight in Sugar Son. Fe-sufficient Sugar Bon inoculated with T22 showed a significant increase in root dry weight relative to other treatment groups (Supplementary Fig. S1D). Furthermore, Sugar Snap experienced significant declines in root length and root dry weight under Fe-deficient conditions, but T22 markedly improved these traits in Fe-deficient conditions (Supplementary Fig. S1C-1D).

Shoot height and shoot dry weight showed no significant changes due to Fe deficiency in Lillian. However, both traits caused a significant decrease when T22 was inoculated both under Fe-deficient and Fe-sufficient conditions (Supplementary Fig. S1E-S1F). Little Marvel showed a significant reduction in shoot height and shoot dry weight under Fe deficiency supplemented with or without T22 relative to Fe-sufficient controls (Supplementary Fig. S1E-1F). Fe-sufficient Little Marvel inoculated with T22 showed similar shoot height and shoot dry weight to the control (Supplementary Fig. S1E-S1F). Also, the shoot height in Green Arrow did not significantly differ across all treatments (Supplementary Fig. S1E-S1F). However, the shoot dry weight in this cultivar showed a significant decline under Fe deficiency either inoculated with T22 or not compared to Fe-sufficient plants. Fe-sufficient plants inoculated with T22 showed a significant increase in shoot dry weight relative to Fe-deficient plants in the absence or presence of T22 (Supplementary Fig. S1E-S1F). In Sugar Bon, shoot length and shoot dry weight were significantly reduced under Fe-deficiency relative to controls. Fe-deficient plants inoculated with T22 showed a significant increase in shoot dry weight but not in shoot height compared to Fe-deficient conditions. However, T22 inoculated under Fe deficiency caused a significant increase in both shoot length and shoot dry weight to that of Fe-deficient plants (Supplementary Fig. S1E-S1F). Sugar Snap exhibited a significant decline in shoot height and shoot dry weight under Fe-deficient conditions compared to controls. However, T22 inoculated under Fe deficiency caused a significant increase in these traits relative to Fe-deficient conditions. Sugar Snap inoculated with T22 with Fe sufficiency showed a similar shoot height and shoot dry weight to those of controls (Supplementary Fig. S1E-S1F).

3.2 Effect of T22 on photosynthetic parameters and rhizosphere siderophore

In this study, Fe deficiency led to substantial retardation in aboveground shoot and belowground root system in Sugar Snap (Fig. 1A-1B). However, plants inoculated with T22 with or without Fe deficiency showed a substantial increase in aboveground and belowground growth relative to the plants solely cultivated with Fe deficiency (Fig. 1A-1B). We measured the leaf chlorophyll fluorescence indices which showed significant variations in response to differential Fe availability in the presence or absence of T22 inoculum (Fig. 1C-1E). We found that Fv/Fm significantly declined in leaves of Sugar Snap due to Fe deficiency compared to the control. The addition of T22 in Fe-deficient soil caused a significant increase in Fv/Fm relative to Fe-starved plants. Plants inoculated with T22 with sufficient Fe showed similar Fv/Fm to that of Fe-sufficient controls (Fig. 1C). Also, Pi_ABS showed a significant decrease in response to Fe deficiency. However, the

addition of T22 with or without Fe deficiency caused a significant increase in Pi_ABS in leaves in comparison to Fe-deficient plants (Fig. 1D).

We also determined the colonization efficiency of T22 in different root partitions of Sugar Snap inoculated with T22 cultivated under Fe deficiency. We found that the meristematic zone (type C) showed a significant increase in the relative abundance of *TaAOX1* compared to the other root partitions (mature zone, elongation zone, root tips) of Sugar Snap (Fig. 1E). Furthermore, siderophore analysis showed that Fe deficiency caused a significant increase in siderophore (%) in rhizosphere soil relative to Fe-sufficient controls (Fig. 1F). Interestingly, Fe-deficient plants inoculated with T22 showed a significant increase in siderophore (%) in rhizosphere soil in contrast to the plants solely grown in Fe-deficient soil. The addition of T22 in soil without Fe deficiency showed a similar siderophore (%) to that of controls but it was significantly lower than Fe-deficient conditions in the absence or presence of T22 inoculum (Fig. 1F).

3.3 Changes in elemental content in plant tissues

During Fe deficiency, the concentration of Fe was significantly reduced in both the roots and leaves of plants as compared to Fe-sufficient controls (Table 1). With the application of T22 to Fe-deficient plants, there was a significant increase in Fe levels in both the roots and leaves of plants relative to plants grown in Fe-deficient conditions. In addition, the concentrations of Zn and B were significantly lower in the roots of plants grown in Fe-deficient conditions as compared to plants grown in Fe-sufficient conditions. The supplementation of T22 in both Fe-deficient and Fe-sufficient plants did not improve Zn and B levels in roots. Also, the concentration of both Zn and B was unchanged in the leaves of plants grown in all four treatments (Table 1). Mn levels were significantly lower in both the roots and leaves of Fe-deficient plants than in plants grown in controls. However, Fe-deficient plants inoculated with T22 exhibited a significant increase in Mn compared to Fe-starved plants. Fe-sufficient plants inoculated with T22 showed equivalent Mn levels to controls (Table 1). The S content was significantly reduced in both the roots and leaves of Fe-deficient plants compared to controls. Also, no significant changes were observed in S levels when Fe-deficient plants were supplemented with T22. T22 inoculated in Fe-sufficient conditions showed similar S in roots to those of plants but leaves still showed a significant decrease compared to controls (Table 1). ICP-MS analysis showed no significant differences in Mg and P concentrations in both roots and leaves of plants regardless of Fe availability and T22 supplementation. Lastly, we found there were no changes in Ca levels in the roots regardless of the different treatment groups. In leaves, Ca levels were significantly reduced under Fe-deficient conditions relative to controls. However, Fe-deficient plants supplementation with T22 showed a significant increase in Ca levels compared to the plants solely cultivated under Fe deficiency. Fe-sufficient plants inoculated with T22 demonstrated similar S levels in leaves to those of controls (Table 1).

3.4 Determination of signaling cascade facilitating symbiotic association

We have successfully established a split-root system to investigate local versus systemic signaling driving the symbiosis between T22 and Sugar Snap under Fe deficiency (Fig. 2A-2B). In this study, garden pea (Sugar Snap) cultivated without T22 in both compartments (+/+) showed significant retardation in shoot growth under Fe deficiency compared to Fe-sufficient controls (Fig. 2C). However, plants inoculated with T22 in both compartments (+/+) or one compartment (-/+) showed significant improvement in shoot growth compared to Fe-deficient plants without T22 in any

compartment (-/-). Interestingly, no phenotypic difference in shoot growth was observed between plants inoculated with T22 in both compartments (+/+) or just one compartment (-/+) (Fig. 2C). Similarly, plants cultivated without Fe deficiency, whether inoculated with T22 in both compartments or just one, showed no significant differences in shoot phenotype compared to plants cultivated under control conditions (Fig. 2C). Under Fe deficiency, plants grown without T22 in both compartments (-/-) exhibited a marked decrease in chlorophyll levels compared to those grown under Fe-sufficient conditions (Fig. 2D). Plants inoculated with T22 in either both compartments (+/+) or a single compartment (-/+) demonstrated significantly higher chlorophyll levels in their leaves compared to Fe-deficient plants that were not inoculated with T22 in any compartment (-/-). However, plants inoculated with T22 in only one compartment (-/+) showed relatively lower ($P<0.05$) chlorophyll levels in their leaves compared to plants inoculated in both compartments (+/+) (Fig. 2D). Lastly, plants cultivated without Fe deficiency, whether inoculated with T22 in both compartments (+/+) or just one (-/+), showed similar leaf chlorophyll levels to those cultivated under control conditions (Fig. 2D).

Plants grown under Fe deficiency without T22 in both compartments (-/-) had significantly lower Fv/Fm and Fe levels in leaves relative to Fe-deficient plants (Fig. 2E-2F). Pea plants cultivated under Fe deficiency or not inoculated with T22 in both compartments (+/+) or one compartment (-/+) showed a significant increase in leaf Fv/Fm and Fe compared to Fe-deficient plants that were not inoculated with T22 (Fig. 2E-2F). Furthermore, plants grown under Fe deficiency without T22 in either compartment (-/-) showed a significant decrease in shoot dry weight and shoot height compared to Fe-deficient plants treated with T22 (Fig. 2G-2H). However, the addition of T22 to either both compartments or a single compartment in plants exposed to Fe deficiency caused a significant improvement in shoot dry weight and shoot height compared to non-inoculated Fe-deficient plants. Furthermore, T22 inoculated in either both compartments or one compartment with sufficient Fe in the soil showed similar shoot dry weight and shoot height to those of control plants (Fig. 2G-2H). Lastly, root length did not show any significant changes regardless of the presence of T22 inoculum in different compartments, with or without Fe deficiency (Fig. 2I).

3.5 Effect of T22 in root transcriptome under Fe deficiency

We performed the RNA-seq analysis to explore the biological involvement of T22 in roots of Sugar Snap exposed to Fe deficiency. RNA-seq analysis in NovaSeq 6000 (PE 150 bp) platform detected 38,048 and 814 genes located in coding and non-translating genes located in garden pea genome (Fig. 3A). Principal component analysis (PCA) indicated that the first principal component (PC1) explained 43.2% of the variance, while the second principal component (PC2) explained 15.9% of the variance (Fig. 3B), suggesting a significant portion of the variability among the sample groups. The RNA-seq analysis revealed that Fe deficiency caused significant (a fold-change threshold ≥ 2, $p \leq 0.05$) changes in the transcriptome in roots of garden pea, with 364 genes exhibiting significant upregulation and 478 genes showing significant downregulation (Fig. 3C and 3D). Relative to Fe-started plants, Fe-deficient plants inoculated with T22 exhibited significant upregulation and downregulation of 575 and 818 genes, respectively. Between Fe-TA+ and Fe- conditions, only 3 overlapping genes showed differential upregulation, while 60 showed differential downregulation. Plants with sufficient Fe levels and inoculated with T22 showed 417 genes upregulated and 379 genes downregulated in the roots, with 54 genes shared in the upregulated category and 165 genes shared in the downregulated category. Furthermore, 442 genes were significantly upregulated, and

367 genes were significantly downregulated in plants inoculated with T22 under sufficient Fe conditions compared to plants inoculated with T22 under Fe deficiency (Fig. 3C-3D).

We further annotated the functions of DEGs using the Ensembl Genomes 58 database for the pea genome and summarized the top candidate genes associated with Fe deficiency tolerance induced by T22 into three categories (Fig. 3E). Among the genes associated with symbiosis and phytohormone signaling, the expression of *Psat5g201640* (monooxygenase activity), *Psat3g072160* (ammonia-lyase activity), *Psat3g201240* (UDP-glycosyltransferase activity), *Psat2g001960* (ammonia-lyase activity), *Psat1g068400* (UDP-glycosyltransferase activity), *Psat7g063080* (UDP-glycosyltransferase activity), *Psat1g006320* (auxin-responsive protein), *Psat2g188920* (4-coumarate A ligase), *Psat7g116000* (monooxygenase activity), and *Psat5g190680* (ABC-type transporter activity) showed significant upregulation in the roots of plants inoculated with T22 compared to Fe-deficient conditions (Fig. 3E). However, some of these genes either remained unchanged or were significantly downregulated (*Psat5g201640*, *Psat3g072160*, *Psat3g201240*, *Psat1g068400*, *Psat7g063080*) due to Fe deficiency compared to controls.

In this study, several candidate genes were significantly upregulated in Fe-deficient plants inoculated with T22 relative to Fe-deficient plants which include: *Psat6g141240* (manganese ion binding), *Psat3g159880* (Fe ion binding), *Psat4g113000* (nitrate transporter activity), *Psat5g286200* (Fe ion binding), *Psat4g000120* (inorganic phosphate transporter), *Psat2g189680* (Zn ion binding), *Psat1g123040* (magnesium ion binding), *Psat1g086520* (oxidoreductase activity), *Psat1g011640* (metal ion transporter activity), *Psat1g171760* (metal ion binding). Most of these transcriptomes showed significant changes in expression due to Fe deficiency. However, *Psat1g086520* (oxidoreductase activity) and *Psat1g011640* (metal ion transporter activity) genes showed a significant downregulation while *Psat5g286200* (Fe ion binding) was significantly increased due to T22 under Fe shortage relative to the Fe-starved plants inoculated with T22 (Fig. 43).

We also found that the expression of *Psat1g168800* (peroxidase activity), *Psat3g121200* (peroxidase activity), *Psat2g065320* (glutamyl−tRNA reductase activity), *Psat3g020440* (*glutathione peroxidase activity*), *Psat5g186720* (meristem development), *Psat5g198360* (glutathione S-transferase), *Psat7g008120* (calcium ion binding), *Psat2g172320* (growth factor activity), *Psat7g008720* (*pyrophosphatase activity*), *Psat2g173800* (peroxidase activity) which are related to growth and redox regulation significantly induced in roots of Fe-deficient plants inoculated with T22 in contrast to Fe-deprived plants. While *Psat2g065320*, *Psat3g020440*, *Psat5g186720*, *Psat1g002320*, *Psat7g008120*, *Psat7g008720* and *Psat2g173800* showed significant downregulation, the rest of the genes showed no significant changes due to Fe deficiency related to controls (Fig. 4E). Furthermore, there were no significant changes in the expression levels of any of top genes discussed under three categories in roots of plants inoculated with T22 under sufficient Fe conditions relative to Fe deficiency (Fig. 3E; Supplementary Table S3).

Analysis of the biological significance of DEGs induced by T22

We have analyzed the biological significance of DEGs in roots of Fe-deficient Sugar Snap inoculated with T22 using ShinyGO (v. 0.80) Bioinformatics Tool (Fig. 4A-4D). Several pathways

significantly enriched were associated with the upregulated DEGs, including but not limited to various biological processes (response to stimulus, organic acid catabolic process, L-phenylalanine catabolic process), molecular functions (ammonia-lyase activity, heme binding), and cellular components (intracellular organelles, organelle) in plants (Fig. 4A-4C). Furthermore, several KEGG pathways were enriched due to differentially expressed genes that were significantly upregulated (flavonoid biosynthesis, biosynthesis of secondary metabolites, phenylalanine metabolism, phenylpropanoid biosynthesis, isoflavonoid biosynthesis) and downregulated (plant-pathogen interaction, MAPK signaling pathway-plant, plant hormone signal transduction, and ribosome) when Fe-deficient plants were inoculated with T22 (Fig. 4D). Furthermore, the gene enrichment analysis of co-expressed network of upregulated DEGS also revealed several key pathways with varying degrees of enrichment and statistical significance. The most significantly enriched pathway was photosynthesis-antenna proteins, followed by phenylpropanoid biosynthesis and biosynthesis of secondary metabolites with moderate enrichment, while isoflavonoid biosynthesis and homologous recombination showed the lowest significance (Supplementary Fig. S4).

3.6 Effect of cinnamic acid on the response of Fe-deficient pea plants

Since RNA-seq revealed the potential role of flavonoid biosynthesis in T22-mediated mitigation of Fe deficiency, we further conducted a targeted study to determine whether cinnamic acid could result in elevated flavonoid levels without exogenous T22 and induce Fe deficiency tolerance in pea plants. We found that Fe-deficient plants had a significantly lower chlorophyll score and Fv/Fm ratio compared to the controls. However, the chlorophyll score and Fv/Fm of plants treated with cinnamic acid or T22 inoculum, whether in the presence or absence of Fe deficiency, were statistically similar to the control plants (Fig. 5A-5B). Plant height and plant dry weight also declined due to Fe deficiency. However, Fe-deficient pea plants supplemented with T22 or cinnamic acid showed a significant increase in plant height and plant dry weight relative to Fe-deficient plants. T22 or cinnamic acid applied to Fe-sufficient plants showed a similar plant height and plant dry weight to those of controls (Fig. 5C-5D). We also measured the siderophore in rhizosphere soil which resulted in a significant increase due to Fe deficiency compared to Fe-sufficient controls (Fig. 5E). Further, Fe-deficient plants supplemented with either T22 or cinnamic acid showed a significant increase in siderophore levels in the rhizosphere compared to Fe-deficient conditions. Interestingly, siderophore levels showed a similar trend when plants were cultivated with sufficient Fe supplemented with T22 or CA to those of control conditions (Fig. 5E). In addition, the total flavonoid content in roots showed no significant changes under Fe deficiency relative to controls (Fig. 5F), while it showed a significant increase when Fe-deficient plants were inoculated with T22. Interestingly, T22-supplemented Fe-sufficient plants showed a significant reduction in flavonoids compared to all other treatments. As expected, the addition of cinnamic acid with or without Fe deficiency showed the highest flavonoid levels in roots which are significantly higher than plants cultivated with or without Fe deficiency in the absence or presence of T22 inoculum (Fig. 5F).

3.7 Changes in nodulation and rhizobia dynamics in roots nodules

The number of root nodules significantly declined under Fe-deficient conditions compared to the control. However, when T22 was added under both Fe-deficient and Fe-sufficient conditions, the number of root nodules significantly increased, returning to levels similar to the control (Fig. 6A). Principal component analysis (PCA) showed large variations (88.4%), resulting in distinct

separations of sample groups (Fig. 6B). In this study, we also analyzed species richness, diversity and relative abundance of 16S bacterial communities in root nodules. We found that species richness (Chao1) and species diversity (Shannon index) showed a significant variation in bacterial communities in root nodules of garden pea cultivated with or without Fe deficiency in the presence or absence of T22 inoculum (Fig. 6C-6D).

Nanopore sequencing showed the differential relative abundance of bacterial genera with an abundance of *Rhizobium* genus in root nodules due to Fe deficiency and T22 inoculum (Fig. 6E). In 16S analysis, the relative abundance of the *Rhizobium* genus substantially decreased in nodules due to Fe deficiency but notably increased when T22 was supplemented in Fe-deficient soil. Furthermore, inoculation with T22 under Fe-sufficient conditions resulted in a relative abundance of *Rhizobium* similar to that of the controls (Fig. 6E). Furthermore, *Sinocapsa* and *Crinalium* showed no substantial changes in root nodules between the control and Fe-deficient soil, inoculated with or without T22. However, plants inoculated with T22 under Fe-sufficient conditions showed a slight increase in the relative abundance of *Sinocapsa* and *Crinalium* in the nodules (Fig. 6E). However, we observed no changes in the abundance of *Gloeobacter*, *Microcoleus*, *Nodosilinea*, *Oculatella*, *Oscillatoria*, and *Pseudanabaena* in nodules, regardless of the availability of Fe or T22 inoculation in the soil (Fig. 6E). Since *Rhizobium* species are key elements in legume nodulation, we further narrowed our analysis down to the species level. We found that the relative abundance of *R. indicum*, *R. leguminosarum*, and *R. redzepovicii* was significantly decreased in root nodules under Fe-deficiency relative to Fe-sufficient controls (Fig. 6F). However, Fe-starved plants inoculated with T22 showed a substantial increase in the relative abundance of *R. leguminosarum*, and *R. redzepovicii* compared to Fe-deficient conditions. Moreover, plants grown under Fe-sufficient conditions exhibited comparable abundances of *R. indicum*, *R. leguminosarum*, and *R. redzepovicii* in root nodules, similar to Fe-sufficient controls (Fig. 6F).

Fe-deficiency caused a significant decrease in the expression of *NifA* and *NifD* relative to controls. However, Fe-deficient pea plants inoculated with T22 showed a significant increase in *NifA* and *NifD* expression compared to Fe-starved plants (Fig. 6G-6H). Fe-sufficient plants supplemented with T22 showed a similar expression levels in *NifA* and *NifD* in nodules to those of controls. Furthermore, the expression of *NifH* significantly increased due to Fe deficiency compared to controls with or without T22. The addition of T22 to Fe-deficient plants showed a significant increase in *NifH* expression in nodules relative to Fe-deficient plants (Fig. 6I).

3.8 Changes in plant responses supplemented with organic Fe

We cultivated Sugar Snap pea plants for 5 weeks to compare the responses of Fe-deficient plants treated with T22 and Fe-supplement (FeEDDHA) supplements. We found that the leaf chlorophyll score significantly declined due to Fe deficiency relative to controls, but the addition of either FeEDDHA or T22 inoculum in the soil caused a significant increase in the chlorophyll score compared to Fe-deficient plants (Fig. 7A). T22 inoculated in Fe-sufficient soil showed a similar chlorophyll score in leaves to that of controls and Fe-deficient plants supplemented with FeEDDHA. Fe-sufficient plants supplemented with FeEDDHA exhibited a significantly higher chlorophyll score than any other treatment group (Fig. 7A). While Fe deficiency caused a significant decrease in plant height and biomass in pea plants, the addition of T22 or FeEDDHA significantly increased these morphological traits relative to plants cultivated solely under Fe

deficiency (Fig. 7B-7C). Fe-sufficient plants supplemented with T22 or FeEDDHA showed similar plant height and biomass to that of controls and Fe-deficient plants supplemented with FeEDDHA (Fig. 7B-7C).

Analysis of rhizosphere siderophore showed a significant decrease due to Fe deficiency compared to controls (Fig. 7D). Moreover, plants deficient in Fe and inoculated with T22 exhibited a significant increase in siderophore levels compared to those grown solely under Fe-deficient and Fe-sufficient conditions. Interestingly, Fe-deficient plants supplemented with FeEDDHA showed a marked decrease in siderophore levels compared to the control, Fe-deficient, and Fe-T22+ conditions. In Fe-sufficient plants inoculated with T22, siderophore levels in the rhizosphere were comparable to those observed in Fe-sufficient controls. However, FeEDDHA supplemented in Fe-sufficient soil showed significantly lower siderophore levels in the rhizosphere compared to all other treatment groups (Fig. 7D). In this study, total flavonoid content in the roots showed no significant changes due to Fe deficiency. However, Fe-deficient plants inoculated with T22 showed a significant increase in flavonoid content relative to plants cultivated solely in Fe-sufficient and Fe-deficient soil (Fig. 7E). Interestingly, Fe-deficient plants treated with FeEDDHA and Fe-sufficient plants supplemented with either T22 or FeEDDHA showed a significant decrease in flavonoid content relative to the other three treatment groups (control, Fe, and Fe-TA+) in roots of pea plants (Fig. 7E). Furthermore, leaf nitrogen content significantly declined due to Fe shortage relative to controls (Fig. 7F). Fe-deficient plants treated either with T22 or FeEDDHA showed a significant increase in nitrogen content compared to Fe-deficient plants. Lastly, Fe-sufficient plants either inoculated with T22 or supplemented with FeEDDHA showed similar nitrogen content in the leaves of pea plants to that of controls (Fig. 7F).

We further studied the interaction of T22 and *R. leguminosarum* in response to differential Fe availability in the nutrient media. The growth of T22 and *R. leguminosarum* significantly decreased when co-cultured together compared to when they were cultivated alone in Fe-sufficient nutrient media (Supplementary Fig. S5). Under Fe deficiency, the growth of T22 showed no significant changes when cultured alone compared to when co-cultivated with *R. leguminosarum*. However, the growth of *R. leguminosarum* significantly increased when co-cultured with T22 in Fe-deficient media compared to when it was cultured alone (Supplementary Fig. S5).

4. DICUSSION

Soil mineral deficiency is a significant challenge in agriculture, often leading to stunted plant growth and reduced yields. Traditional methods to improve plant stress tolerance, such as genetic modification and chemical fertilizers (Yadav et al. 2023; Guzmán et al. 2022), often fall short in sustainability and long-term effectiveness. A microbiome-aided approach, particularly by beneficial microorganisms like T22 offers a sustainable alternative to improve crop resilience to Fe deficiency (Kabir et al. 2022; Zhao et al. 2020). This study provides the first mechanistic evidence of how T22 interacts with the host to establish a symbiotic relationship, modulate the host transcriptome, and influence nodule microbial dynamics, thereby aiding garden peas to cope with Fe-deprived conditions.

4.1 The colonization efficiency of T22 in mitigating Fe deficiency is host-specific:

Fungal colonization in plant roots is highly host-specific and is driven by various factors, including host genetics, immune responses, and the compatibility of fungal species with the host plant's

physiology (Morán-Diez et al. 2015; Liu et al. 2019). In this study, the abundance analysis of *TaAOX1* showed that only Sugar Bon and Sugar Snap Cultivars exhibited a significant abundance of fungal colonization in their roots. This suggests a potential genetic basis for host-specific interactions, which could be leveraged to improve fungal symbiosis and stress tolerance in microbiome-efficient cultivars. More specifically, Sugar Snap inoculated with T22 showed the highest abundance being consistent with the improved efficiency in photosynthetic attributes in leaves under Fe deficiency, which further decreased substantially when Fe availability in the soil was adequate. This indicates that the beneficial effects of T22 may be dependent on the plant's Fe status, highlighting the complex interaction between the fungus, the plant, and nutrient availability in the soil. Morán-Diez et al. (2015) analyzed the transcriptomic response of *T. virens* during interactions with maize and tomato roots. They found 35 genes that were significantly differentially expressed between the two hosts, with 10 showing higher expression when in contact with tomato roots compared to maize. In this study, we partitioned the root system of Sugar Snap into sections, resulting in the highest colonization efficiency of T22 in its meristematic zone as evident in the higher abundance of *TaAOX1*. The root meristematic zone offers abundant nutrients, exudates, and a favorable microenvironment, enhancing the efficiency of microbial colonization compared to other root segments (Tsai et al. 2023; Canarini et al. 2019). In addition, the root system is crucial for plant fitness, enabling water and mineral absorption, with fungal colonization varying across root segments (Kabir and Bennetzen 2024; López-Bucio et al. 2003). As a result, the high abundance of T22 in the meristematic zone of garden peas, which we further considered for downstream RNA-seq experiments. The high abundance of T22 in the meristematic zone may be associated with active cell division and growth, providing optimal conditions for this fungal species (Russo et al. 2019). Thus, these findings emphasize the need for cultivar screening favorable for T22 colonization is crucial for optimizing plant-microbe interactions and promoting stress resilience in crops.

4.2 Systemic signaling modulated by host flavonoid promotes symbiosis

Microbial networks enable the exchange of signals and cues among plants, inducing plant responses to cope with environmental changes (Gorzelak et al. 2015). Symbiotic signaling between microbes and plants exposed to abiotic stress is essential for mediating beneficial interactions that improve plant fitness and resilience. In this study, a split-root assay revealed that the presence of T22 in the rhizosphere, even when split into two distinct compartments, is not necessary to induce Fe deficiency tolerance in garden pea. The study found that tolerance to Fe deficiency in Sugar Snap remained unaffected by the absence of T22 inoculation in one of the compartments. This suggests that the mechanism through which T22 induces Fe deficiency tolerance in garden pea relies on signals triggered by the host plant itself, rather than local signals within the rhizosphere. Yet, the source of signals that aid colonization is influenced by host genetics, typically linked to the secretion of metabolites and responses to environmental cues (Wiesmann et al. 2023; Bapaume and Reinhardt 2012).

Our RNA-seq analysis of the meristematic segment of roots revealed the upregulation of several key genes associated with symbiosis when Fe-deficient pea plants were inoculated with T22. We found the induction of genes responsible for monooxygenase activity, ammonia-lyase activity, auxin-responsive protein, and 4-coumarate A ligase in the roots of Fe-deficient Sugar Snap inoculated with T22. In plants, monooxygenase enzymes play a multifaceted role in facilitating and maintaining symbiotic relationships between plants and microorganisms. Studies suggest that

monooxygenase activity is involved in signaling, secondary metabolite production, and hormone regulation that may contribute significantly to the health and resilience of plants in symbiotic systems (Wu et al. 2020; Mnguni et al. 2020; Dasgupta et al. 2011). Particularly, ammonia-lyase enzymes, especially phenylalanine ammonia-lyase (PAL), play significant roles in the symbiotic relationships between plants and microorganisms (Liu et al. 2023). PAL is a crucial enzyme in the phenylpropanoid pathway that converts phenylalanine to cinnamic acid which is then transformed into 4-coumarate, involved in the biosynthesis pathway of coumarins and flavonoids in plants (Li et al. 2020). Coumarins, synthesized via the phenylpropanoid pathway in plants, act as signaling molecules regulating interactions between symbiotic microbes and plants (Harbort et al. 2020; Stringlis et al. 2009). In Fe-deficient plants, 4-coumarate is crucial for enhancing Fe uptake in non-grass plants when Fe is deprived in soil (Paffrath et al. 2024). They reported that Fe-deprived *Arabidopsis* plants coordinate coumarin (i.e. fraxetin) biosynthesis to optimize Fe acquisition. Further, coumarins can modify the root microbiota and exhibit a widespread yet strain-specific commensal trait that addresses Fe deficiency in Arabidopsis (Harbort et al. 2020). Also, flavonoids released by plants have been found to promote microbial colonization and serve as pre-symbiotic signaling molecules in microbial-plant symbiosis (Lidoy et al. 2023; Schliemann et al. 2008). We found consistency in the genes induced in the root by T22 with the KEGG pathway analysis, which also showed enrichment in the biosynthesis pathways of flavonoid, isoflavonoid, and phenylpropanoid biosynthesis. Flavonoids play a crucial role in rhizobia nodulation in legume crops by acting as signaling molecules that attract rhizobia to the root (Wang et al. 2018). NodD proteins in rhizobia are tailored to recognize specific flavonoids secreted by legumes, establishing an early checkpoint in symbiosis (Peck et al. 2006). Additionally, flavonoids serve as antioxidants in plants, offering protection against a range of environmental stresses (Grace 2000). Thus, our findings suggest that the induction of ammonia-lyase activity and 4-coumarate A ligase in roots of pea plants mediated by T22 may play essential roles in the initial steps of flavonoid biosynthesis by producing key intermediates. This may lead to the formation of various flavonoid compounds to promote symbiotic association with T22 and/or rhizobia in helping pea plants cope with Fe deficiency.

Flavonoid accumulation in plants is influenced by the regulation of genes involved in the flavonoid biosynthetic pathway (Borevitz et al. 2000). Therefore, we conducted a targeted study on the effect of cinnamic acid (precursor of flavonoid biosynthesis) to further validate the role of flavonoids in a possible symbiotic relationship with soil microbes, underlying Fe deficiency tolerance in pea plants. In this study, pea plants inoculated with T22 or supplemented with cinnamic acid showed equally significant improvement in photosynthetic parameters and plant biomass compared to Fe-deficient plants. Interestingly, this improvement in plant health correlated with increased synthesis of rhizosphere siderophores and flavonoids in roots. This suggests that elevated flavonoid levels may induce the release of siderophores by rhizosphere microbes, ultimately promoting the solubilization of insoluble Fe to help pea plants cope with stress. Zamboni et al. (2012) observed that tomato plants respond to Fe deficiency by upregulating the flavonoid-3-hydroxylase gene, suggesting an additional role for flavonoids in influencing Fe bioavailability in soil. In light of this knowledge, future work may develop biotechnological approaches, such as transgenic plants or microbial inoculants, to enhance the expression of key flavonoid biosynthesis genes or to optimize T22 colonization for improved Fe acquisition in garden pea and other legume crops.

4.3 Reversal of Fe-deficiency-induced retardation in mineral and redox status

Once the symbiotic relationship between a plant and microbe is established, host plants reprogram their responses to varying degrees to cope with abiotic stress. In the present study, garden pea plants with Fe deficiency exhibited reduced chlorophyll scores and decreased photosynthetic efficiency in their leaves, consistent with findings from previous studies on legume crops exposed to Fe deficiency (Haque et al. 2022; Kabir et al. 2012). Aligned with the morphological improvement, our study demonstrated that the inoculation of T22 resulted in a significant improvement in chlorophyll synthesis and photosynthetic performance in pea plants exposed to Fe deficiency. Previous studies have reported enhanced chlorophyll scores, photosystem II activity, and photosynthesis performance index following the application of T22 to plants deficient in minerals (Kabir and Bennetzen 2024; Kabir et al. 2022; Singh et al. 2019). In our study, we observed that T22 inoculation mitigated morphological and physiological damage in Fe-deficient pea plants, consistent with increased Fe concentrations in both roots and shoots. Additionally, supplementation of T22 under Fe-deficient conditions significantly restored Mn levels in plants. Studies showed that the application of *Trichoderma* strains resulted in elevated Fe levels but reduced concentrations of Cu, Mn, and Zn in some plants grown in calcareous soils (Kabir and Bennetzen 2024; Santiago et al. 2011). The differential levels of minerals in plants inoculated with *Trichoderma* may be attributed to variations in mineral forms and alterations in metal transporter activity in host plants (Ye et al. 2017). However, the enhancement of Fe and Mn status in garden pea exposed to Fe deficiency by T22 underscores its potential impact on inducing transporters crucial for nutrient acquisition, as evidenced by the upregulation of several genes in roots observed in RNA-seq analysis. Our RNA-seq analyses identified genes responsible for manganese ion binding, Fe ion binding, and metal ion binding that were either downregulated or showed no change in expression but were substantially induced by T22 under Fe-deficient conditions. Different plant cultivars display varying degrees of resistance to Fe deficiency, influenced by diverse mechanisms of homeostasis and gene expression patterns observed over different timeframes under stress conditions (Atencio et al. 2021; Kabir et al. 2012). In this study, pea plants deficient in Fe and inoculated with T22 exhibited the upregulation of Fe-related genes (*Psat3g159880*, *Psat5g286200*) compared to Fe-deficient plants without inoculation, indicating a symbiotic advantage in enhancing Fe uptake in the rhizosphere. This suggests that Fe-deficient plants either sense the need to increase Fe uptake or are compelled to induce Fe uptake when insoluble Fe(III) is solubilized through microbial interactions in the rhizosphere. This can be explained by the elevated siderophore levels in the rhizosphere when plants were deficient in Fe, with the highest levels observed when T22 was supplemented. When plants are deficient in Fe, there is typically an increase in siderophores in the rhizosphere, secreted by both bacterial and fungal communities, to chelate Fe (Jin et al. 2010; Crowley et al. 2006). Harzianic acid, a secondary metabolite produced by T22, has been demonstrated to bind with Fe(III), thereby enhancing the solubilization of Fe in the soil environment. This process benefits both other microorganisms and the host plant (Vinale et al. 2013). Yet, the quantity of siderophores released by *Trichoderma* during its interaction with host plants varies with the host Cultivar, as supported by our findings (Fig. 1A). Thus, it implies that elevated siderophore levels in the Fe-deficient rhizosphere soil may be associated with exogenous T22, as evidenced by its highest colonization efficiency in the roots of Sugar Snap under such conditions.

The accumulation of reactive oxygen species (ROS) induced by Fe deficiency results in oxidative damage to cellular components including lipids, proteins, and DNA (Tewari et al. 2013). Given

779 that Fe is essential for primary antioxidant enzymes, oxidative damage in plants is exacerbated
780 under conditions of Fe deficit (Halliwell, 2006). While Fe-deficient pea plants exhibited induction
781 of mineral transporters due to T22, they also demonstrated upregulation of several peroxidase and
782 glutathione-related genes, suggesting that this symbiotic association might be coupled with the
783 induction of ROS scavenging in Fe-starved sorghum. While the mechanistic basis for how ROS
784 balance is modulated in plants with mycorrhizal associations remains limited, multiple studies
785 have demonstrated the role of AMF and *Trichoderma* in inducing antioxidants to protect plants
786 from abiotic stressors including Fe deficiency (García-Sanchez et al. 2014; Kabir and Bennetzen,
787 2024). Furthermore, it is documented that flavonoids play a crucial role as antioxidants,
788 detoxifying and scavenging ROS produced as by-products of oxidative metabolism (Jan et al.
789 2021; Nakabayashi et al. 2014). However, Mastouri et al. (2012) demonstrated that in drought-
790 stressed tomato plants colonized with T22, there was an enhanced ability to scavenge ROS and
791 recycle oxidized forms of ascorbate and glutathione, which contributed to the improvement of
792 ROS-scavenging pathways. In another study, T22 enhanced antioxidant defense in Fe-deficient
793 soybeans by boosting glutathione reductase activity and increasing glutathione and methionine to
794 stabilize the redox state (Kabir et al. 2022). While the mechanistic role of T22 in ROS scavenging
795 requires further study, T22-mediated elevated flavonoid may likely influence the reprogramming
796 of ROS homeostasis in pea plants exposed to Fe deficiency.
797
798 Maintaining ROS balance can improve photosystem II efficiency, ensuring better light capture and
799 energy conversion in plants exposed to abiotic stress (Nadarajah 2020), and support meristem
800 development by minimizing cellular damage (Huang et al. 2019). Excessive buildup of ROS,
801 especially in photosystems I and II, can lead to damage of Fe-S proteins, essential cofactors in
802 plant photosynthesis (Xiong et al. 2021; Murchie and Niyogi 2011). Our findings indicate that Fe
803 deficiency resulted in reduced chlorophyll synthesis and decreased Fv/Fm in the leaves of garden
804 pea. Since Fe-deficient pea inoculated with T22 substantially improved Fe and ROS status, genes
805 related to photosystem II (*Psat1g002320*) and meristem development (*Psat5g186720*) were
806 consistently upregulated under these conditions. This molecular evidence was supported by
807 improved leaf Fv/Fm ratios and root systems in plants supplemented with T22 under Fe deficiency.
808 Research has shown that mycorrhizal symbiosis mediated by AMF in *Robinia pseudoacacia*
809 enhances PSII activity in chloroplasts, leading to improved water use efficiency (Yang et al. 2015).
810 Additionally, studies have shown that T22 can restore chlorophyll levels and photosystem II
811 activity in other mineral-deficient plants (Kabir et al. 2022; Singh et al. 2019). Our study suggests
812 that T22 may play a crucial role in enhancing photosynthetic efficiency, potentially by indirectly
813 modulating ROS homeostasis.
814
815 **4.4 T22 restores nodule bacterial dynamics in pea exposed to Fe deficiency**
816 Rhizobia is essential for the growth and stress resilience of legume crops, as they form symbiotic
817 relationships that enhance nitrogen fixation and improve overall plant health under various stress
818 conditions (Shumilina et al. 2023). Given the observed changes in nodulation and expression of
819 nitrogen-fixation genes, we further investigated whether T22 impacts the bacterial diversity and
820 dynamics in root nodules of pea plants exposed to Fe deficiency. Our results demonstrate that Fe
821 deficiency leads to a marked reduction in the number of root nodules. However, the addition of
822 T22 not only mitigated the negative effects of Fe deficiency but also enhanced nodule formation
823 under both Fe-deficient and Fe-sufficient conditions. This suggests a potential biostimulant effect
824 of T22 on nodule development. The synergistic effects of *Rhizobium* and mycorrhizal interactions

825 are still not fully understood. However, rhizobia and AMF can form symbioses with legumes,
826 significantly enhancing plant mineral nutrition, particularly nitrogen and phosphorus uptake
827 (Ossler et al. 2015; Xie et al. 2018). In this study, microbiome analysis in pea nodules showed
828 substantial changes in species richness and diversity in response to Fe availability and T22
829 inoculation. These findings highlight the profound impact of both Fe deficiency and T22
830 inoculation on the overall bacterial community structure within root nodules in pea plants. Fe is
831 essential for the functioning of nitrogenase, the enzyme complex responsible for nitrogen fixation
832 in legume plant nodules (Schwember et al. 2019; Brear et al. 2013). Nanopore sequencing further
833 elucidated the changes in the relative abundance of bacterial genera, particularly focusing on the
834 *Rhizobium*. The inoculation of pea plants with T22 significantly increased the relative abundance
835 of *Rhizobium* in Fe-deficient soils. These findings suggest the positive impact of T22 on restoring
836 beneficial *Rhizobium* populations under Fe stress, thereby promoting nodulation and overall plant
837 health of peas exposed to Fe deficiency. However, it is unknown at this point whether the improved
838 nodule formation is a direct consequence of T22 on Rhizobia or the effect of the improved nutrient
839 status of Fe-deficient pea plants indirectly mediated by T22. Although Rhizobia-fungi symbiotic
840 associations share common signals and processes, mycorrhizal symbiosis has been reported to
841 increase phosphorus content. This can boost nitrogenase enzyme activity, leading to higher
842 nitrogen fixation by rhizobial symbionts, and, in return, better mycorrhizal development (Ren et
843 al. 2016; Hao et al. 2019). Additionally, AMF can reduce oxidative stress in the nodules (Porcel et
844 al. 2003) and enhance the carbon metabolism within them (Goicoechea et al. 2004). Furthermore,
845 fungi can produce and modulate plant hormones, which promote root and nodule development
846 (Chanclud and Morel 2016).

847 We further conducted a targeted study to elucidate whether T22-mediated mitigation of Fe
848 deficiency in pea plants is directly related to associations with rhizosphere microbes, including
849 rhizobia, or indirectly linked to the improved Fe status of the plants. Fe fertilizers are commonly
850 used to prevent the precipitation of Fe in the soil, ensuring its availability even in alkaline or
851 calcareous soils, leading to healthier, more vigorous plant growth and increased yields
852 (Schenkeveld et al. 2010). In this study, we found that both T22 and FeEDDHA were equally
853 effective in mitigating the retardation of chlorophyll synthesis and plant biomass caused by Fe
854 deficiency in pea plants. However, we observed differences in rhizosphere siderophore and root
855 flavonoid content; both showed a simultaneous decrease when Fe-deficient pea plants were
856 supplemented with FeEDDHA compared to plants inoculated with T22. It suggests that the
857 mechanisms by which these treatments mitigate Fe deficiency in pea plants differ. Specifically, it
858 implies that T22 was involved with siderophore production and host flavonoid content, potentially
859 enhancing the plant's own Fe acquisition processes, while FeEDDHA primarily provides a direct
860 source of available Fe without stimulating these secondary metabolic pathways. Microbial
861 siderophore production is closely linked to Fe availability in the soil (Timofeeva et al. 2022). When
862 soil Fe levels are low, microorganisms increase siderophore production to scavenge Fe more
863 effectively and make it available to both microbes and plants (Ahmed and Holmström 2014). Kabir
864 and Bennetzen (2024) showed that Fe deficiency significantly increased the siderophore-related
865 (*SIT1*) gene in T22, resulting in the solubilization of Fe, which improved Fe status in sorghum.
866 They found the highest siderophore accumulation in sorghum inoculated with T22 under Fe-
867 deficient conditions compared to plants grown with sufficient Fe. Consistently, the elevated

868 siderophore released by T22 in the rhizosphere of Fe-deficient pea plants may be no longer needed
869 when organic Fe fertilizer is available. However, the elevation of siderophore in the rhizosphere
870 of Fe-deficient plants suggests that not only T22 but also other microbes may be involved. Several
871 studies support the idea that bacterial communities, including rhizobia, release siderophores in
872 response to Fe deficiency, thereby improving Fe uptake by plants alongside other beneficial
873 interactions such as nitrogen fixation (Lurthy et al. 2020; Wang et al. 2024; Brear et al. 2013).

874 Our follow-up study further demonstrated that Fe-deficient pea plants were able to combat
875 deficiency symptoms with Fe supplementation, without increasing rhizosphere siderophore and
876 root flavonoid content, which is a requirement for T22-mediated improvement of Fe status. The
877 initiation of a complex legume-rhizobium development begins with the release of flavonoids
878 (Dong and Song 2020). Since siderophores and flavonoids are involved in symbiotic associations,
879 Fe-deficient plants bypassed this strategy by overcoming Fe deficiency when organic Fe was
880 supplemented in the soil. When Fe is sufficient, bacteria may prioritize other metabolic processes
881 over nodulation to conserve energy which helps them efficiently allocate resources based on
882 environmental cues, enhancing their overall fitness (Frawley and Fang 2014). Therefore, our
883 findings suggest that the presence of T22, rather than Fe status alone, may be involved in restoring
884 rhizobia dynamics under Fe-deficient conditions, contributing to the mechanistic pathways that
885 mitigate Fe deficiency in pea plants. Therefore, T22 may enhance nodulation and support Fe
886 uptake through specific mechanisms that go beyond simply altering the Fe status of the plants.
887 This result is preliminary given the complexity of the soil system, which shapes multifactorial
888 effects on Fe-deficient pea plants. However, our *in vitro* study demonstrated the positive effect of
889 T22 on the growth of *R. leguminosarum* in Fe-deficient nutrient media. These results are consistent
890 with our overall study on the role of T22 in restoring rhizobia dynamics in nodules of Fe-deficient
891 plants. So far, there is a lack of well-documented interaction between T22 and rhizobia in scientific
892 literature. However, it is known that *Trichoderma* can enhance the activities of beneficial bacteria
893 such as *Pseudomonas* or *Bacillus*, which contribute to improved plant health and nutrient uptake
894 (Poveda et al. 2022; da Costa et al. 2022). *Trichoderma* species are known to produce a variety of
895 metabolites that can play a role in shaping the composition and dynamics of soil or rhizosphere
896 bacterial communities, influencing overall ecosystem health and plant-microbe interactions (Gao
897 et al. 2023). This correlates with the levels of flavonoids in roots, as rhizobia are also attracted to
898 flavonoid-mediated symbiosis (Shumilina et al. 2023; Li et al. 2019). Furthermore, *Trichoderma*
899 application has been found to shift in other fungal communities in the rhizosphere (Asghar and
900 Kataoka 2021; Umadevi et al. 2018). Future research could explore how T22 interacts with
901 rhizobia and identify the specific metabolites responsible for this association in legume plants
902 under varying Fe availability conditions.

903 **CONCLUSION**

904 This study unveils the intricate mechanisms by which T22 interacts with both garden pea hosts
905 and the rhizobia community to mitigate Fe deficiency. We demonstrated that T22 enhances plant
906 health parameters under Fe deficiency by improving tissue Fe levels and elevating rhizosphere
907 siderophores, critical for Fe uptake. Furthermore, T22 fosters the 16S microbial community,
908 particularly enhancing rhizobia abundance and upregulating essential nitrogen fixation genes in
909 nodules (Fig. 8). Our findings underscore systemic signaling pathways between T22 and host
910 plants, promoting Fe deficiency tolerance across different root compartments. RNA-seq analysis

revealed significant gene expression changes linked to flavonoid biosynthesis, mineral transport, and redox homeostasis in T22-inoculated pea roots under Fe deficiency. Moreover, the restoration of plant health with cinnamic acid in the absence of T22 reinforces the role of flavonoids in promoting microbial symbiosis. However, the substitution of T22 with Fe supplementation reduced siderophore and flavonoid levels, nullifying the associations of microbiome-dominated Fe improvement. Overall, our mechanistic insights highlight the potential of T22 as a key player in microbiome-based strategies to alleviate Fe deficiency in legume crops, paving the way for sustainable agricultural practices. These insights provide a valuable foundation for developing strategies to improve legume growth and stress resilience through targeted microbial interventions.

ACKNOWLEDGMENTS

We express our gratitude to the Genomics Core of Michigan State University. This research was supported by a startup grant (5SFAES-293007) and Elizabeth and Hayden Cutler Endowed Professorship in Biotechnology from the University of Louisiana at Monroe.

AUTHOR CONTRIBUTION

AT was involved in experimental design, plant cultivation, RNA extraction, RNA-seq data analysis, data collection, interpretation, and 16S data analysis. Md Rokibul Hasan assisted with DNA extraction and microbial co-culture experiments. AHK provided overall supervision, guidance in experimental design, data interpretation, and manuscript revision.

CONFLICT OF INTEREST

We have no conflict of interest.

DATA AVAILABILITY

The data supporting the findings of this study are available in the article and its supplementary information files. Also, the sequencing data used and described in this study has been uploaded to NCBI under the Bioproject accession numbers: PRJNA1133893 (RNA-seq) and PRJNA1134200 (16S).

REFERENCES

Ahmed, E., and Holmström, S. J. (2014). Siderophores in environmental research: roles and applications. Microbial biotechnology, 7(3), 196–208.

Alcántara, E., Romera, F. J., Canete, M., and De la Guardia, M. D. (2000). Effects of bicarbonate and Fe supply on Fe (III) reducing capacity of roots and leaf chlorosis of the susceptible peach rootstock "Nemaguard." Journal of Plant Nutrition, 23(11–12), 1607–1617.

Anders, S., Pyl, P.T., Huber, W., 2015. HTSeq–a Python framework to work with high-throughput sequencing data. Bioinformatics 31 (2), 166–169.

Asghar, W., and Kataoka, R. (2021). Effect of co-application of *Trichoderma* spp. with organic composts on plant growth enhancement, soil enzymes and fungal community in soil. Archives of microbiology, 203(7), 4281–4291.

Atencio, L.A., Salazar, J.S., Lauter, A.N.M., Gonzales, M.D., O'Rourke, J.A., Graham, M.A., 2021. Characterizing short- and long-term Fe stress responses in Fe deficiency tolerant and susceptible soybean (*Glycine max* L. Merr.). Plant Stress 2, 100012.

Bapaume, L., and Reinhardt, D. (2012). How membranes shape plant symbioses: signaling and transport in nodulation and arbuscular mycorrhiza. Frontiers in plant science, 3, 223.

Bhardwaj, D., Ansari, M.W., Sahoo, R.K., Tuteja, N., 2014. Biofertilizers function as key players in sustainable agriculture by improving soil fertility, plant tolerance, and crop productivity. Microb. Cell Fact. 13, 66.

Bjørk, P. K., Johansen, N. T., Havshøi, N. W., Rasmussen, S. A., Ipsen, J. Ø., Isbrandt, T., Larsen, T. O., and Fuglsang, A. T. (2023). *Trichoderma harzianum* peptaibols stimulate plant plasma membrane H+-ATPase activity. ACS Omega, 8(38), 34928–34937.

Boeglin, L., Morère Le-Paven, M. C., Clochard, T., Fustec, J., and Limami, A. M. (2022). Pisum sativum Response to Nitrate as Affected by *Rhizobium leguminosarum*-derived signals. Plants (Basel, Switzerland), 11(15), 1966.

Bolger, A.M., Lohse, M., Usadel, B., 2014. Trimmomatic: a flexible trimmer for Illumina Sequence Data. Bioinforma. btu170.

Borevitz, J.O.; Xia, Y.J.; Blount, J.; Dixon, R.A.; Lamb, C. Activation tagging identifies a conserved MYB regulator of phenylpropanoid biosynthesis. Plant Cell 2000, 12, 2383–2393.

Brear, E. M., Day, D. A., and Smith, P. M. (2013). Fe: an essential micronutrient for the legume-rhizobium symbiosis. Frontiers in plant science, 4, 359.

Brear, E. M., Day, D. A., and Smith, P. M. (2013). Fe: an essential micronutrient for the legume-rhizobium symbiosis. Frontiers in plant science, 4, 359.

Bucher M., Hause B., Krajinski F., Küster H. (2014). Through the doors of perception to function in arbuscular mycorrhizal symbioses. New Phytol. 204: 833–840.

Canarini, A., Kaiser, C., Merchant, A., Richter, A., and Wanek, W. (2019). Root exudation of primary metabolites: mechanisms and their roles in plant responses to environment stimuli. Frontiers in plant science, 10, 157.

Chanclud, E., and Morel, J. B. (2016). Plant hormones: a fungal point of view. Molecular plant pathology, 17(8), 1289–1297.

Chaudhari D, Rangappa K, Das A, Layek J, Basavaraj S, Kandpal BK, Shouche Y, Rahi P. Pea (Pisum sativum l.) plant shapes its rhizosphere microbiome for nutrient uptake and stress amelioration in acidic soils of the North-East Region of India. Front Microbiol. 2020 Jun 3;11:968.

Clarke, J.D., 2009. Cetyltrimethyl ammonium bromide (CTAB) DNA miniprep for plant DNA isolation. Cold Spring Harb. Protoc., pdb.prot5177

Connorton, J. M., Balk, J., and Rodríguez-Celma, J. (2017). Fe homeostasis in plants - a brief overview. Metallomics : integrated biometal science, 9(7), 813–823.

Crowley D.E. Microbial siderophores in the plant rhizosphere. In: Barton L.L., Abadia J., editors. Fe Nutrition in Plants and Rhizospheric Microorganisms. Springer; Dordrecht, The Netherlands: 2006. pp. 169–198.

Curie, C. and Mari, S. (2017) New routes for plant Fe mining. New Phytol, 214(2), 521–525.

da Costa SDA, Cardoso AF, de Castro GLS, Junior DDS, da Silva TC, da Silva GB. 2022. Co-Inoculation of *Trichoderma asperellum* with *Bacillus subtilis* to promote growth and nutrient absorption in Marandu Grass. https://doi.org/10.1155/2022/3228594

Dasgupta, K., Ganesan, S., Manivasagam, S., and Ayre, B. G. (2011). A cytochrome P450 monooxygenase commonly used for negative selection in transgenic plants causes growth anomalies by disrupting brassinosteroid signaling. BMC plant biology, 11, 67.

Dixon R., Kahn D. (2004). Genetic regulation of biological nitrogen fixation. Nat. Rev. Microbiol. 2 621–631

Dong, W., and Song, Y. (2020). The Significance of flavonoids in the process of biological nitrogen fixation. International journal of molecular sciences, 21(16), 5926.

Frawley, E. R., and Fang, F. C. (2014). The ins and outs of bacterial iron metabolism. Molecular microbiology, 93(4), 609–616.

Gao, P., Qi, K., Han, Y., Ma, L., Zhang, B., Zhang, Y., Guan, X., and Qi, J. (2023). Effect of *Trichoderma viride* on rhizosphere microbial communities and biocontrol of soybean root rot. Frontiers in microbiology, 14, 1204688.

García-S´anchez, M., Palma, J.M., Ocampo, J.A., García-Romera, I., Aranda, E., 2014. Arbuscular mycorrhizal fungi alleviate oxidative stress induced by ADOR and enhance antioxidant responses of tomato plants. J. Plant Physiol. 171 (6), 421–428.

Ge, S.X., Jung, D., Yao, R., 2020. ShinyGO: a graphical gene-set enrichment tool for animals and plants. Bioinformatics 36 (8), 2628–2629.

Giovannetti, M., Binci, F., Navazio, L., and Genre, A. (2024). Nonbinary fungal signals and calcium-mediated transduction in plant immunity and symbiosis. The New phytologist, 241(4), 1393–1400.

Goicoechea, N.; Merino, S.; Sanchez-Diaz, M. Contribution of arbuscular mycorrhizal fungi (AMF) to the adaptations exhibited by the deciduous shrub *Anthyllis cytisoides* L. under water deficit. Physiol. Plant. 2004, 122, 453–464.

Gorzelak MA, Asay AK, Pickles BJ, Simard SW. 2015. Inter-plant communication through mycorrhizal networks mediates complex adaptive behaviour in plant communities. AoB Plants 7, plv050.

Grace, S.C.; Logan, B.A. Energy dissipation and radical scavenging by the plant phenylpropanoid pathway. Philos. Trans. R. Soc. B 2000, 355, 1499–1510.

Guzmán, M.G, Cellini, F., Fotopoulos, V., Balestrini, R., and Arbona, V. (2022). New approaches to improve crop tolerance to biotic and abiotic stresses. Physiologia plantarum, 174(1), e13547.

Hacisalihoglu, G., Beisel, N. S., and Settles, A. M. (2021). Characterization of pea seed nutritional value within a diverse population of *Pisum sativum*. PloS one, 16(11), e0259565.

Halliwell, B., 2006. Reactive species and antioxidants. Redox biology is a fundamental theme of aerobic life. Plant Physiol. 141 (2), 312–322.

Hao Z, Xie W, Jiang X, Wu Z, Zhang X, Chen B. Arbuscular mycorrhizal fungus improves *Rhizobium*–Glycyrrhiza seedling symbiosis under drought stress. Agronomy. 2019; 9(10):572.

Haque, A. F. M. M., Rahman, M. A., Das, U., Rahman, M. M., Elseehy, M. M., El-Shehawi, A. M., Parvez, M. S., and Kabir, A. H. (2022). Changes in physiological responses and MTP (metal tolerance protein) transcripts in soybean (*Glycine max*) exposed to differential Fe availability. Plant physiology and biochemistry, 179, 1–9.

Harbort, C. J., Hashimoto, M., Inoue, H., Niu, Y., Guan, R., Rombolà, A. D., Kopriva, S., Voges, M. J. E. E. E., Sattely, E. S., Garrido-Oter, R., and Schulze-Lefert, P. (2020). Root-secreted coumarins and the microbiota interact to improve Fe nutrition in Arabidopsis. Cell host and microbe, 28(6), 825–837.e6.

Harbort, C. J., Hashimoto, M., Inoue, H., Niu, Y., Guan, R., Rombolà, A. D., Kopriva, S., Voges, M. J., Sattely, E. S., and Garrido-Oter, R. (2020). Root-secreted coumarins and the microbiota interact to improve Fe nutrition in Arabidopsis. Cell Host and Microbe, 28(6), 825–837.

Harman, G. E., Howell, C. R., Viterbo, A., Chet, I., and Lorito, M. (2004). *Trichoderma* species-opportunistic, avirulent plant symbionts. Nature Reviews Microbiology, 2(1), 43–56.

Hider, R.C., Kong, X., 2010. Chemistry and biology of siderophores. Nat. Prod. Rep. 27 (5), 637–657.

Himpsl, S.D., Mobley, H.L.T., 2019. Siderophore Detection Using Chrome Azurol S and cross-feeding assays. Met. Mol. Biol. 2021, 97–108.

Hu, K., 2021. Become competent in generating RNA-seq heat maps in one day for novices without prior R experience. Met. Mol. Biol. 2239, 269–303.

Huang, H., Ullah, F., Zhou, D. X., Yi, M., and Zhao, Y. (2019). Mechanisms of ROS Regulation of Plant Development and Stress Responses. Frontiers in plant science, 10, 800.

Jan, R., Kim, N., Lee, S. H., Khan, M. A., Asaf, S., Lubna, Park, J. R., Asif, S., Lee, I. J., and Kim, K. M. (2021). Enhanced favonoid accumulation reduces combined salt and heat stress through regulation of transcriptional and hormonal mechanisms. Frontiers in plant science, 12, 796956.

Jin, C. W., Li, G. X., Yu, X. H., and Zheng, S. J. (2010). Plant Fe status affects the composition of siderophore-secreting microbes in the rhizosphere. Annals of botany, 105(5), 835–841.

Kabir, A. H., and Bennetzen, J. L. (2024). Molecular insights into the mutualism that induces iron deficiency tolerance in sorghum inoculated with *Trichoderma harzianum*. Microbiological research, 281, 127630.

Kabir, A. H., Paltridge, N. G., Able, A. J., Paull, J. G., and Stangoulis, J. C. (2012). Natural variation for Fe-efficiency is associated with upregulation of Strategy I mechanisms and enhanced citrate and ethylene synthesis in *Pisum sativum* L. Planta, 235(6), 1409–1419.

Kabir, A. H., Rahman, M. A., Rahman, M. M., Brailey-Jones, P., Lee, K. W., and Bennetzen, J. L. (2022). Mechanistic assessment of tolerance to Fe deficiency mediated by *Trichoderma harzianum* in soybean roots. Journal of applied microbiology, 133(5), 2760–2778.

Kabir, A.H., Rahman, M.M., Haider, S.A., Paul, N.K., 2015. Mechanisms associated with differential tolerance to Fe deficiency in okra (*Abelmoschus escu*lentus Moench). EnvFe. Exp. Bot. 112, 16–26.

Kim, D., Langmead, B., Salzberg, S.L., 2015. HISAT: a fast spliced aligner with low memory requirements. Nat. Methods 12 (4), 357–360.

Kroh, G. E., and Pilon, M. (2019). Connecting the negatives and positives of plant Fe homeostasis. The New phytologist, 223(3), 1052–1055.

Li, N., Islam, M. T., and Kang, S. (2019). Secreted metabolite-mediated interactions between rhizosphere bacteria and *Trichoderma* biocontrol agents. PloS one, 14(12), e0227228.

Li, S. S., Chang, Y., Li, B., Shao, S. L., and Zhen-Zhu-, Z. (2020). Functional analysis of 4-coumarate: CoA ligase from Dryopteris fragrans in transgenic tobacco enhances lignin and flavonoids. Genetics and molecular biology, 43(2), e20180355.

Liao, D., Wang, S., Cui, M., Liu, J., Chen, A., and Xu, G. (2018). Phytohormones regulate the development of arbuscular mycorrhizal symbiosis. International journal of molecular sciences, 19(10), 3146.

Lidoy J, Berrio E, García M, España-Luque L, Pozo MJ, López-Ráez JA. (2023). Flavonoids promote *Rhizophagus irregularis* spore germination and tomato root colonization: A target for sustainable agriculture. Frontiers in Plant Science, 5;13:1094194.

Liu, A., Zhu, Y., Wang, Y., Wang, T., Zhao, S., Feng, K., Li, L., and Wu, P. (2023). Molecular identification of phenylalanine ammonia lyase-encoding genes *EfPALs* and *EfPAL2*-interacting transcription factors in Euryale ferox. Frontiers in plant science, 14, 1114345.

Liu, H., Senthilkumar, R., Ma, G., Zou, Q., Zhu, K., Shen, X., Tian, D., Hua, M. S., Oelmüller, R., and Yeh, K. W. (2019). *Piriformospora indica*-induced phytohormone changes and root

colonization strategies are highly host-specific. Plant signaling and behavior, 14(9), 1632688.

Livak KJ, Schmittgen TD. Methods. Vol. 25. San Diego, CA: 2001. Analysis of relative gene expression data using real-time quantitative PCR and the 2(-Delta Delta C(T)) Method; pp. 402–408.

López-Bucio, J., Cruz-Ramírez, A., and Herrera-Estrella, L. (2003). The role of nutrient availability in regulating root architecture. Current opinion in plant biology, 6(3), 280–287.

Lopez-Obando M., Ligerot Y., Bonhomme S., Boyer F.D., Rameau C. (2015). Strigolactone biosynthesis and signaling in plant development. Development 142: 3615–3619.

Lurthy, T., Cantat, C., Jeudy, C., Declerck, P., Gallardo, K., Barraud, C., Leroy, F., Ourry, A., Lemanceau, P., Salon, C., and Mazurier, S. (2020). Impact of bacterial siderophores on Fe status and ionome in Pea. Frontiers in plant science, 11, 730.

MacLean, A. M., Bravo, A., and Harrison, M. J. (2017). Plant signaling and metabolic pathways enabling arbuscular mycorrhizal symbiosis. The Plant cell, 29(10), 2319–2335.

Mastouri, F., Bj¨orkman, T., Harman, G.E., 2012. *Trichoderma harzianum* enhances antioxidant defense of tomato seedlings and resistance to water deficit. Mol. Plant- Micr. Interact 25 (9), 1264–1271.

McMurdie, P. J., and Holmes, S. (2013). phyloseq: an R package for reproducible interactive analysis and graphics of microbiome census data. *PloS One*, *8*(4), e61217.

Mnguni, F. C., Padayachee, T., Chen, W., Gront, D., Yu, J. H., Nelson, D. R., and Syed, K. (2020). More P450s are involved in secondary metabolite biosynthesis in *Streptomyces* compared to *Bacillus*, Cyanobacteria, and Mycobacterium. International journal of molecular sciences, 21(13), 4814.

Molnár, Z., Solomon, W., Mutum, L., and Janda, T. (2023). Understanding the mechanisms of Fe deficiency in the rhizosphere to promote plant resilience. Plants (Basel, Switzerland), 12(10), 1945.

Morán-Diez, M. E., Trushina, N., Lamdan, N. L., Rosenfelder, L., Mukherjee, P. K., Kenerley, C. M., and Horwitz, B. A. (2015). Host-specific transcriptomic pattern of *Trichoderma virens* during interaction with maize or tomato roots. BMC genomics, 16(1), 8.

Murchie, E.H., Niyogi, K.K., 2011. Manipulation of photoprotection to improve plant photosynthesis. Plant Physiol. 155, 86–92.

Nadarajah K. K. (2020). ROS homeostasis in abiotic stress tolerance in plants. International journal of molecular sciences, 21(15), 5208.

Nakabayashi, R., Yonekura-Sakakibara, K., Urano, K., Suzuki, M., Yamada, Y., Nishizawa, T., Matsuda, F., Kojima, M., Sakakibara, H., Shinozaki, K., Michael, A. J., Tohge, T., Yamazaki, M., and Saito, K. (2014). Enhancement of oxidative and drought tolerance in Arabidopsis by overaccumulation of antioxidant flavonoids. The Plant journal, 77(3), 367–379.

Ossler, J. N., Zielinski, C. A., and Heath, K. D. (2015). Tripartite mutualism: facilitation or trade-offs between rhizobial and mycorrhizal symbionts of legume hosts. American journal of botany, 102(8), 1332–1341.

Paffrath, V., Tandron Moya, Y. A., Weber, G., von Wirén, N., and Giehl, R. F. H. (2024). A major role of coumarin-dependent ferric Fe reduction in strategy I-type Fe acquisition in Arabidopsis. The Plant cell, 36(3), 642–664.

Pandey PK, Bhowmik P, Kagale S. Optimized methods for random and targeted mutagenesis in field pea (*Pisum sativum* L.). Front Plant Sci. 2022 Sep 8;13:995542.

1139 Peck, M. C., Fisher, R. F., and Long, S. R. (2006). Diverse flavonoids stimulate NodD1 binding to
1140 nod gene promoters in *Sinorhizobium meliloti*. J. Bacteriol. 188, 5417–5427.
1141 Piyanete, C., Meechai, P. and Nakbanpotecc, W. Antioxidant activities and phenolic contents of
1142 extracts from *Salvinia olesta* and *Eichorniacrassipes*. Res. J. Biol. Sci. 4, 1113–1117 (2009).
1143 Porcel, R.; Barea, J.M.; Ruiz-Lozano, J.M. Antioxidant activities in mycorrhizal soybean plants
1144 under drought stress and their possible relationship to the process of nodule senescence. New
1145 Phytol. 2003, 157, 135–143.
1146 Poveda J, Eugui D. 2022. Combined use of *Trichoderma* and beneficial bacteria (mainly Bacillus
1147 and Pseudomonas): Development of microbial synergistic bio-inoculants in sustainable
1148 agriculture. Biological Control 176, 105100.
1149 Qi, W., and Zhao, L. (2013). Study of the siderophore-producing *Trichoderma asperellum* Q1 on
1150 cucumber growth promotion under salt stress. Journal of Basic Microbiology, 53(4), 355–
1151 364.
1152 Ren, C.G.; Bai, Y.J.; Kong, C.C.; Bian, B.; Xie, Z.H. Synergistic interactions between salt-tolerant
1153 rhizobia and arbuscular mycorrhizal fungi on salinity tolerance of *Sesbania cannabina*
1154 plants. J. Plant Growth Regul. 2016, 35, 1098–1107.
1155 Rodríguez-Celma, J. and Schmidt, W. (2013) Reduction-based Fe uptake revisited: on the role of
1156 secreted Fe-binding compounds. Plant Signal Behav, 8, e26116.
1157 Russo G, Carotenuto G, Fiorilli V, Volpe V, Chiapello M, Van Damme D, Genre A., 2019. Ectopic
1158 activation of cortical cell division during the accommodation of arbuscular mycorrhizal
1159 fungi. New Phytol. 221(2), 1036-1048.
1160 Santiago, A., Quintero, J.M., Aviles, M., Delgado, A., 2011. Effect of *Trichoderma asperellum*
1161 strain T34 on Fe, copper, manganese, and zinc uptake by wheat grown on a calcareous
1162 medium. Plant Soil 342, 97–104.
1163 Schenkeveld, W. D., Reichwein, A. M., Bugter, M. H., Temminghoff, E. J., and van Riemsdijk, W.
1164 H. (2010). Performance of soil-applied FeEDDHA isomers in delivering Fe to soybean plants
1165 in relation to the moment of application. Journal of agricultural and food chemistry, 58(24),
1166 12833–12839.
1167 Schliemann, W., Ammer, C., and Strack, D. (2008). Metabolite profiling of mycorrhizal roots of
1168 *Medicago truncatula*. Phytochemistry, 69(1), 112–146.
1169 Shumilina, J., Soboleva, A., Abakumov, E., Shtark, O. Y., Zhukov, V. A., and Frolov, A. (2023).
1170 Signaling in Legume-Rhizobia Symbiosis. International journal of molecular sciences,
1171 24(24), 17397.
1172 Shumilina, J., Soboleva, A., Abakumov, E., Shtark, O. Y., Zhukov, V. A., and Frolov, A. (2023).
1173 Signaling in Legume-Rhizobia Symbiosis. International journal of molecular sciences,
1174 24(24), 17397.
1175 Singh, S.P., Pandey, S., Mishra, N., Giri, V.P., Mahfooz, S., Bhattacharya, A., Kumari, M.,
1176 Chauhan, P., Verma, P., Nautiyal, C.S., Mishra, A., 2019. Supplementation of *Trichoderma*
1177 improves the alteration of nutrient allocation and transporter genes expression in rice under
1178 nutrient deficiencies. Plant Physiol. Biochem. 143, 351–363.
1179 Singh, S.P., Pandey, S., Mishra, N., Giri, V.P., Mahfooz, S., Bhattacharya, A., Kumari, M.,
1180 Chauhan, P., Verma, P., Nautiyal, C.S., Mishra, A., 2019. Supplementation of *Trichoderma*
1181 improves the alteration of nutrient allocation and transporter genes expression in rice under
1182 nutrient deficiencies. Plant Physiol. Biochem. 143, 351–363.
1183 Stringlis, I. A., de Jonge, R., and Pieterse, C. M. J. (2019). The age of coumarins in plant-microbe
1184 Interactions. Plant and cell physiology, 60(7), 1405–1419.

1185 Sun, C., Wu, T., Zhai, L., Li, D., Zhang, X., Xu, X., Han, Z., 2016. Reactive oxygen species
1186 function to mediate the Fe deficiency response in an Fe-efficient apple Cultivar: An early
1187 response mechanism for enhancing reactive oxygen production. Front. Plant Sci. 7, 1726.
1188 Tewari, R.K., Hadacek, F., Sassmann, S., Lang, I., 2013. Fe deprivation-induced reactive oxygen
1189 species generation leads to non-autolytic PCD in *Brassica napus* leaves. EnvFe. Exp. Bot.
1190 91, 74–83
1191 Thilakarathna, M. S., and Cope, K. R. (2021). Split-root assays for studying legume-rhizobia
1192 symbioses, rhizodeposition, and belowground nitrogen transfer in legumes. Journal of
1193 experimental botany, 72(15), 5285–5299.
1194 Timofeeva, A. M., Galyamova, M. R., and Sedykh, S. E. (2022). Bacterial siderophores:
1195 classification, biosynthesis, perspectives of use in agriculture. Plants (Basel, Switzerland),
1196 11(22), 3065.
1197 Tsai, H. H., Wang, J., Geldner, N., and Zhou, F. (2023). Spatiotemporal control of root immune
1198 responses during microbial colonization. Current opinion in plant biology, 74, 102369.
1199 Umadevi, P., Anandaraj, M., Srivastav, V., and Benjamin, S. (2018). Trichoderma harzianum
1200 MTCC 5179 impacts the population and functional dynamics of microbial community in the
1201 rhizosphere of black pepper (*Piper nigrum* L.). Brazilian journal of microbiology 49(3), 463–
1202 470.
1203 Vert, G., Briat, J.F. and Curie, C. (2001) Arabidopsis *IRT2* gene encodes a root-periphery Fe
1204 transporter. Plant J, 26, 181–189.
1205 Vinale, F., Nigro, M., Sivasithamparam, K., Flematti, G., Ghisalberti, E.L., Ruocco, M., Lorito,
1206 M., 2013. Harzianic acid: a novel siderophore from *Trichoderma harzianum*. FEMS
1207 Microbiol. Lett. 347 (2), 123–129.
1208 Wang, N., Wang, T., Chen, Y., Wang, M., Lu, Q., Wang, K., Dou, Z., Chi, Z., Qiu, W., Dai, J., Niu,
1209 L., Cui, J., Wei, Z., Zhang, F., Kümmerli, R., and Zuo, Y. (2024). Microbiome convergence
1210 enables siderophore-secreting-rhizobacteria to improve Fe nutrition and yield of peanut
1211 intercropped with maize. Nature communications, 15(1), 839.
1212 Wang, Q., Liu, J., and Zhu, H. (2018). Genetic and molecular mechanisms underlying symbiotic
1213 specificity in legume-Rhizobium interactions. Frontiers in plant science, 9, 313.
1214 Wiesmann CL, Wang NR, Zhang Y, Liu Z, Haney CH. 2023. Origins of symbiosis: shared
1215 mechanisms underlying microbial pathogenesis, commensalism and mutualism of plants and
1216 animals. FEMS Microbiology Reviews 47, fuac048.
1217 Wu, H., Zou, Q., Luo, S., He, D., Li, X., Yan, C., and Cheng, G. (2020). Lack of the slavin-
1218 containing monooxygenase FmoA partially impairs the symbiotic interaction of
1219 *Mesorhizobium Huakuii* with *Astragalus Sinicus*. https://doi.org/10.21203/rs.3.rs-27635/v1
1220 Xie, W.; Hao, Z.P.; Zhou, X.F.; Jiang, X.L.; Xu, L.J.; Wu, S.L.; Zhao, A.H.; Zhang, X.; Chen, B.D.
1221 Arbuscular mycorrhiza facilitates the accumulation of glycyrrhizin and liquiritin in
1222 Glycyrrhiza uralensis under drought stress. Mycorrhiza 2018, 28, 285–300.
1223 Xiong, H., Hua, L., Reyna-Llorens, I., Shi, Y., Chen, K.M., Smirnoff, N., Hibberd, J.M., 2021.
1224 Photosynthesis-independent production of reactive oxygen species in the rice bundle sheath
1225 during high light is mediated by NADPH oxidase. PNAS 118, e2022702118
1226 Yadav, R. K., Tripathi, M. K., Tiwari, S., Tripathi, N., Asati, R., Chauhan, S., Tiwari, P. N., and
1227 Payasi, D. K. (2023). Genome editing and improvement of abiotic stress tolerance in crop
1228 plants. Life (Basel, Switzerland), 13(7), 1456.
1229 Yates, A. D., Allen, J., Amode, R. M., Azov, A. G., Barba, M., Becerra, A., Bhai, J., Campbell, L.
1230 I., Carbajo Martinez, M., Chakiachvili, M., Chougule, K., Christensen, M., Contreras-

Moreira, B., Cuzick, A., Da Rin Fioretto, L., Davis, P., De Silva, N. H., Diamantakis, S., Dyer, S., Elser, J., … Flicek, P. (2022). Ensembl Genomes 2022: an expanding genome resource for non-vertebrates. Nucleic acids research, 50(D1), D996–D1003.

Ye, Q., Park, J.E., Gugnani, K., Betharia, S., Pino-Figueroa, A., Kim, J., 2017. Influence of Fe metabolism on manganese transport and toxicity. Metall 16, 1028–1046.

Zamboni, A., Zanin, L., Tomasi, N., Pezzotti, M., Pinton, R., Varanini, Z., et al. (2012). Genome-wide microarray analysis of tomato roots showed defined responses to Fe deficiency. BMC Genomics 13, 101.

Zhao, L., Wang, Y., and Kong, S. (2020). Effects of *Trichoderma asperellum* and its siderophores on endogenous auxin in *Arabidopsis thaliana* under Fe-deficiency stress. International Microbiology, 23(4), 501–509.

Table 1. ICP-MS analysis of nutrients in root and leaf of pea plants inoculated with or without *T. afroharzianum* (TA) in the absence or presence of Fe deficiency in the soil. Data represents ± SD of three independent biological samples. Different letters indicate significant differences between different treatment groups at P < 0.05 level.

Elements	**Root**				**Leaf**			
	Control	Fe-	Fe-TA+	TA+	Control	Fe-	Fe-TA+	TA+
Fe (ppm)	401.0±14.8a	292.9±53.3b	361.1±53.3a	425.7±27.2a	89.5±14.8a	60.5±53.3b	75.3±53.3c	90.1±27.2a
Zn (ppm)	129.5±0.9a	92.5±35.5b	92.0±35.5b	100.3±24.4b	50.1±0.9a	50.6±35.5a	49.4±35.5a	51.0±24.4a
Mn (ppm)	35.9±8.1a	22.7±18.8b	27.8±18.8c	35.9±7.6a	33.8±8.1a	18.6±18.8b	25.3±18.8c	34.6±7.6a
B (ppm)	17.6±0.4a	9.3±6.8b	11.004±6.8b	11.5±4.4b	11.6±0.4a	10.5±6.8a	10.9±6.8a	10.0±4.4a
S (%)	1.06±0.1a	0.80±0.2b	0.87±0.2b	1.15±0.12a	0.55±0.1a	0.28±0.2b	0.38±0.2b	0.37±0.12b
Mg (%)	0.14±0.0a	0.16±0.1a	0.19±0.1a	0.20±0.07a	0.21±0.1a	0.19±0.1a	0.20±0.1a	0.18±0.07a
Ca (%)	0.69±0.3a	0.66±0.5a	0.66±0.5a	0.64±0.11a	1.02±0.3a	0.39±0.5b	0.58±0.5c	1.05±0.11a
P (%)	0.39±0.0a	0.34±0.5a	0.35±0.5a	0.37±0.30a	0.63±0.01a	0.68±0.5a	0.64±0.5a	0.65±0.30a

Supplementary data

Supplementary Table S1. Physico-chemical properties of soil used for the cultivation of pea plants.

Supplementary Table S2. Gene-specific primers used in qPCR experiments.

Supplementary Table S3. The top differentially expressed genes in roots of garden pea and their expression in different growth conditions. Values marked with an asterisk are significant > Log2 fold, < P value 0.05.

Supplementary Fig. S1. Culture of *T. afroharzianum* T22 inoculum in potato dextrose agar (PDA) after 3 days of incubation at 25°C.

Supplementary Fig. S2. Screening of genetic lines sensitive to Fe deficiency but can capitalize T. afroharzianum T22cto combat Fe deficiency. The data presented are means with standard deviations (n = 3 individual replicates). Statistically significant differences among the treatments at a p < 0.05 level were indicated by different alphabetical letters above the bars.

Supplementary Fig. S3. Schematic representation of different root partitions used for the colonization efficiency of T22.

Supplementary Fig. S4. Gene enrichment analysis of co-expressed gene networks of upregulated DEGs in roots pea plants inoculated with T22.

1266 **Supplementary Fig. S5.** Co-culture of *T. afroharzianum* (T22) and *R. leguminosarum* (RL) in
1267 nutrient agar under Fe-sufficient (control and Fe-deficient conditions for 7 days. The data
1268 presented are means with standard deviations (n = 3 individual replicates). Statistically
1269 significant differences among the treatments at a $p < 0.05$ level were indicated by different
1270 alphabetical letters above the bars.

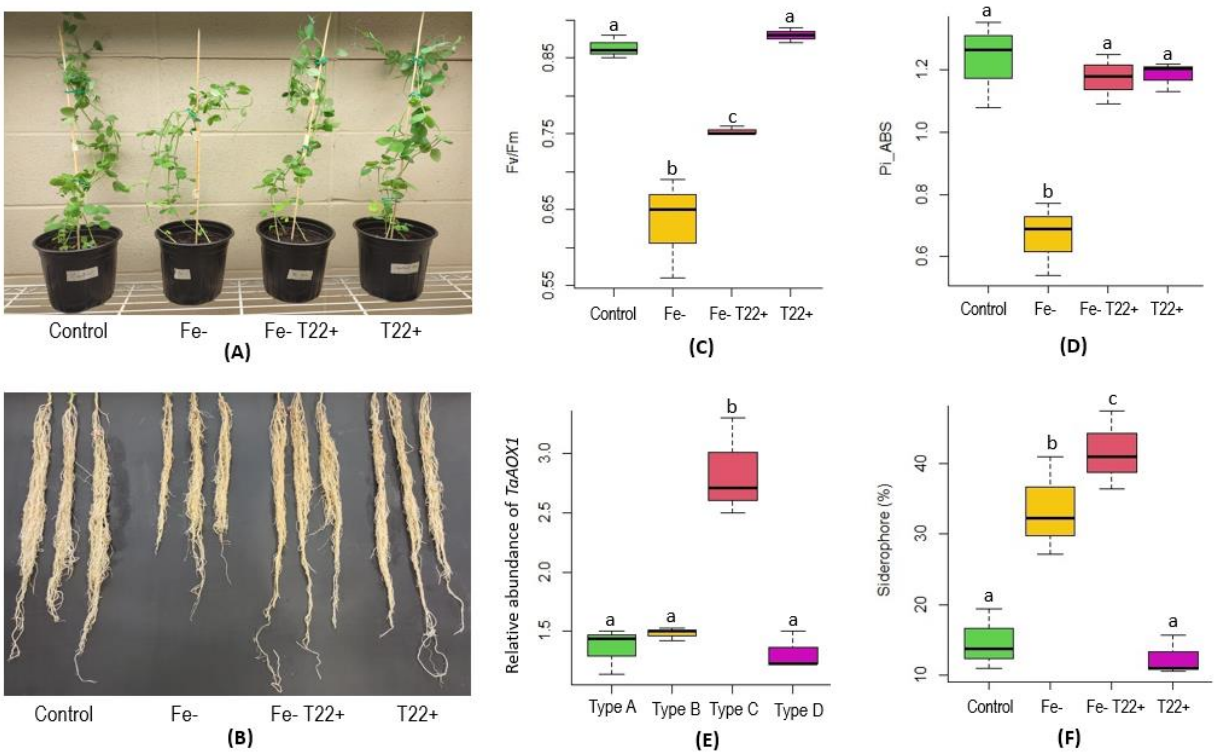

Fig. 1. Changes in aboveground shoot (A), belowground root (B), leaf chlorophyll fluorescence indices: Fv/Fm - maximal quantum yield of PS II (C), Pi_ABS; Pi_ABS - photosynthetic performance index (D), the relative abundance of *TaAOX1* in different root partitions (type A: mature zone, type B: elongation zone, type C: meristematic zone, type D: root tips) of Sugar Snap (E), and siderophore % in rhizosphere soil (F) in Sugar Snap cultivated in the absence (Fe-) or presence (control) of Fe deficiency inoculated with (T22+) or without T22. The data presented are means with standard deviations (n = 3 individual replicates). Statistically significant differences among the treatments at a $p < 0.05$ level were indicated by different alphabetical letters above the bars, where applicable.

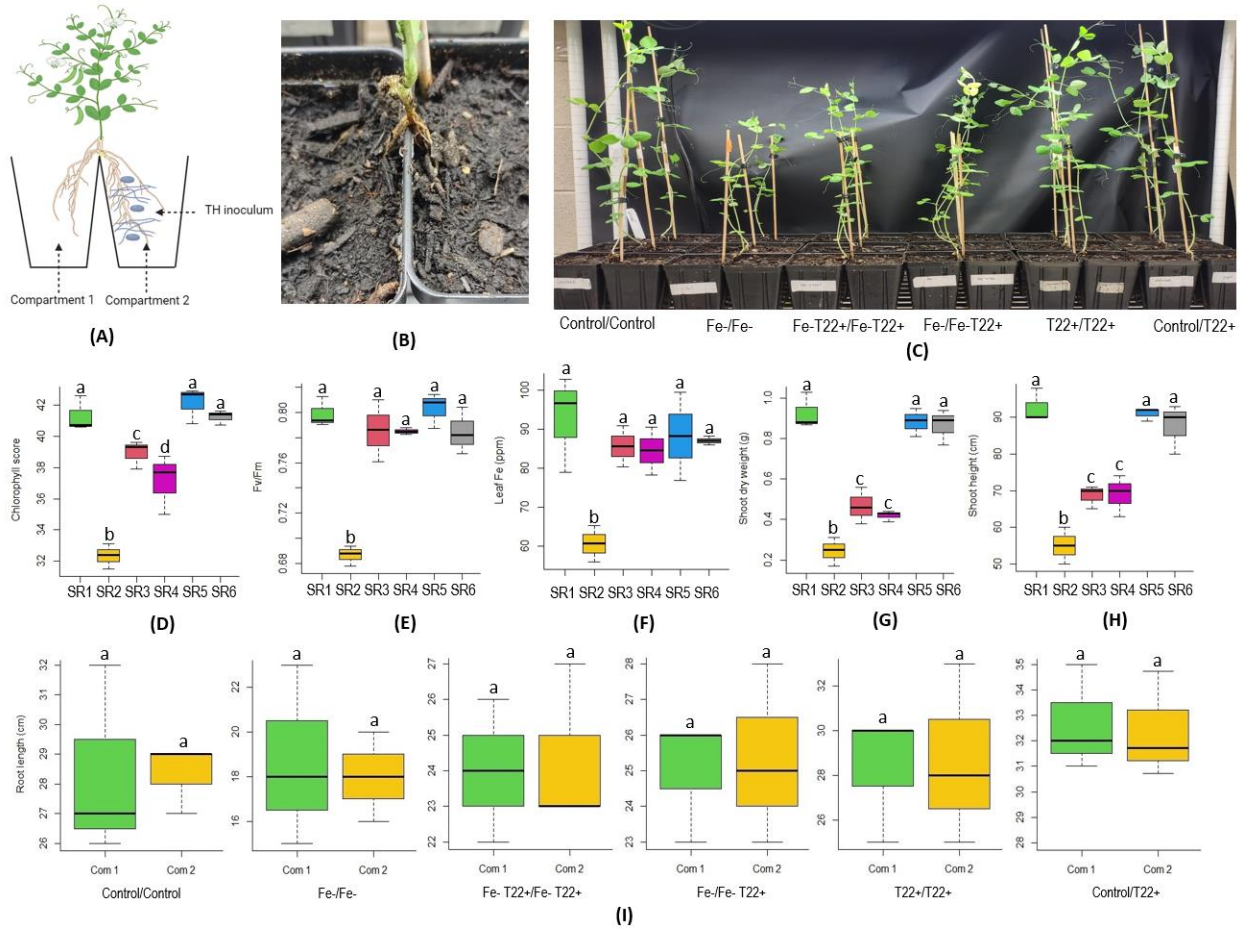

Fig. 2. Schematic diagram of split-root system (A), establishment of split-root (B), plant phenotype (C), leaf chlorophyll score (D), leaf Fv/Fm (E), leaf Fe (F), shoot dry weight (G), shoot height (H) and root length of plants grown in each compartment (I) in the absence or presence of Fe deficiency and T22 inoculum. The data presented are means with standard deviations (n = 3 individual replicates). Statistically significant differences among the treatments at a $p < 0.05$ level were indicated by different alphabetical letters above the bars, where applicable.

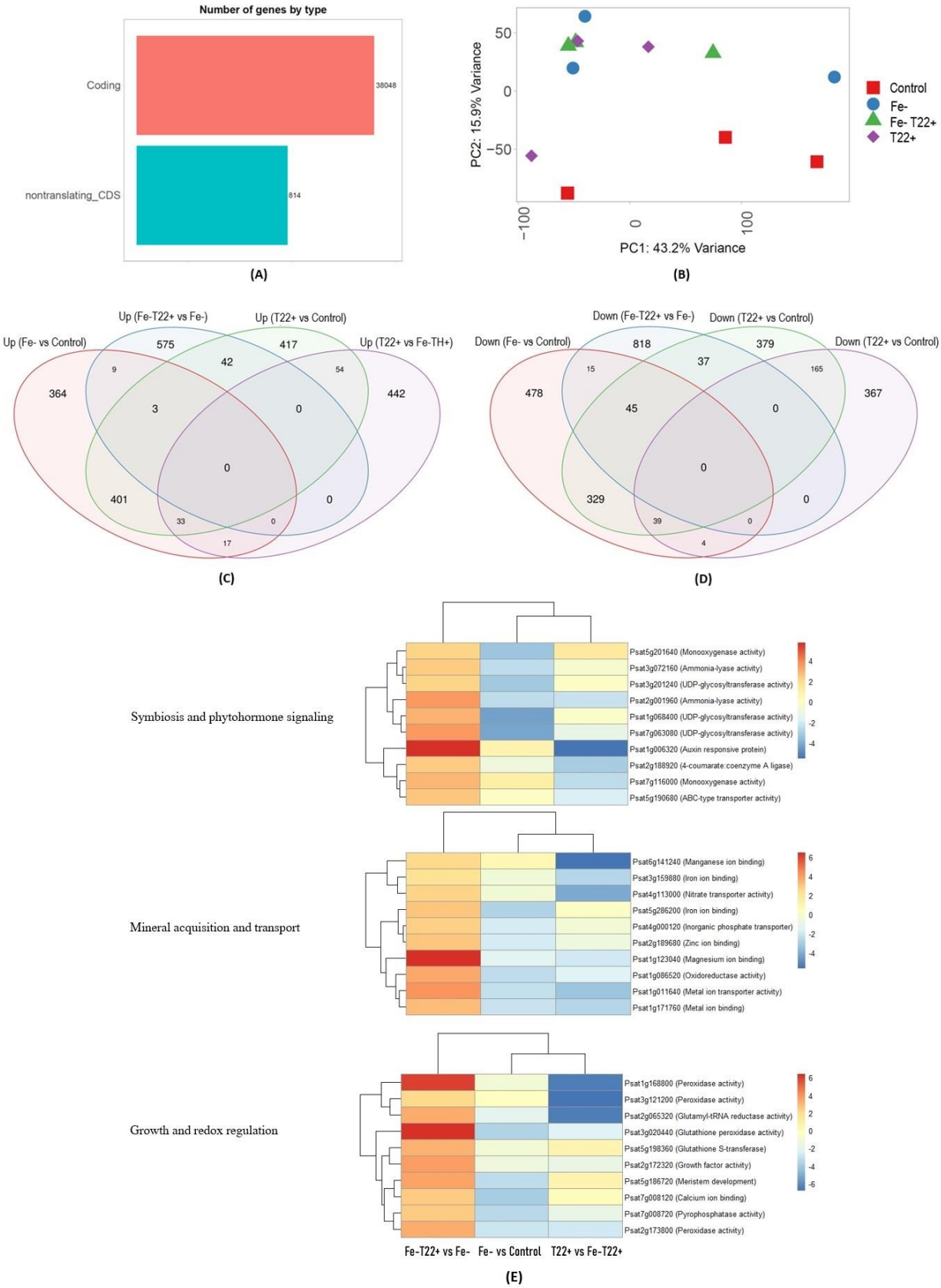
Number of genes by type
Coding
38048
nontranslating_CDS
814
(A)
PC2: 15.9% Variance
PC1: 43.2% Variance
Control
Fe-
Fe- T22+
T22+
(B)
Up (Fe- vs Control)
Up (Fe-T22+ vs Fe-)
Up (T22+ vs Control)
Up (T22+ vs Fe-TH+)
364
575
417
442
9
42
54
3
0
0
401
0
33
0
17
(C)
Down (Fe- vs Control)
Down (Fe-T22+ vs Fe-)
Down (T22+ vs Control)
Down (T22+ vs Control)
478
818
379
367
15
37
165
45
0
0
329
0
39
0
4
(D)
Symbiosis and phytohormone signaling
Psat5g201640 (Monooxygenase activity)
Psat3g072160 (Ammonia-lyase activity)
Psat3g201240 (UDP-glycosyltransferase activity)
Psat2g001960 (Ammonia-lyase activity)
Psat1g068400 (UDP-glycosyltransferase activity)
Psat7g063080 (UDP-glycosyltransferase activity)
Psat1g006320 (Auxin responsive protein)
Psat2g188920 (4-coumarate:coenzyme A ligase)
Psat7g116000 (Monooxygenase activity)
Psat5g190680 (ABC-type transporter activity)
Mineral acquisition and transport
Psat6g141240 (Manganese ion binding)
Psat3g159880 (Iron ion binding)
Psat4g113000 (Nitrate transporter activity)
Psat5g286200 (Iron ion binding)
Psat4g000120 (Inorganic phosphate transporter)
Psat2g189680 (Zinc ion binding)
Psat1g123040 (Magnesium ion binding)
Psat1g086520 (Oxidoreductase activity)
Psat1g011640 (Metal ion transporter activity)
Psat1g171760 (Metal ion binding)
Growth and redox regulation
Psat1g168800 (Peroxidase activity)
Psat3g121200 (Peroxidase activity)
Psat2g065320 (Glutamyl-tRNA reductase activity)
Psat3g020440 (Glutathione peroxidase activity)
Psat5g198360 (Glutathione S-transferase)
Psat2g172320 (Growth factor activity)
Psat5g186720 (Meristem development)
Psat7g008120 (Calcium ion binding)
Psat7g008720 (Pyrophosphatase activity)
Psat2g173800 (Peroxidase activity)
Fe-T22+ vs Fe-
Fe- vs Control
T22+ vs Fe-T22+
(E)

Fig. 3. RNA-seq analysis: number of gene readings by their type (A), principal component analysis of gene variation (B), Venn diagram of differentially expressed ((> Log2 fold, < P value 0.05)) upregulated (C) and downregulated (D) genes and heatmap of top 10 upregulated genes (E) associated with different functions (symbiosis and phytohormone signaling, mineral acquisition and transport and growth and redox regulations) in pea plants inoculated with T22.

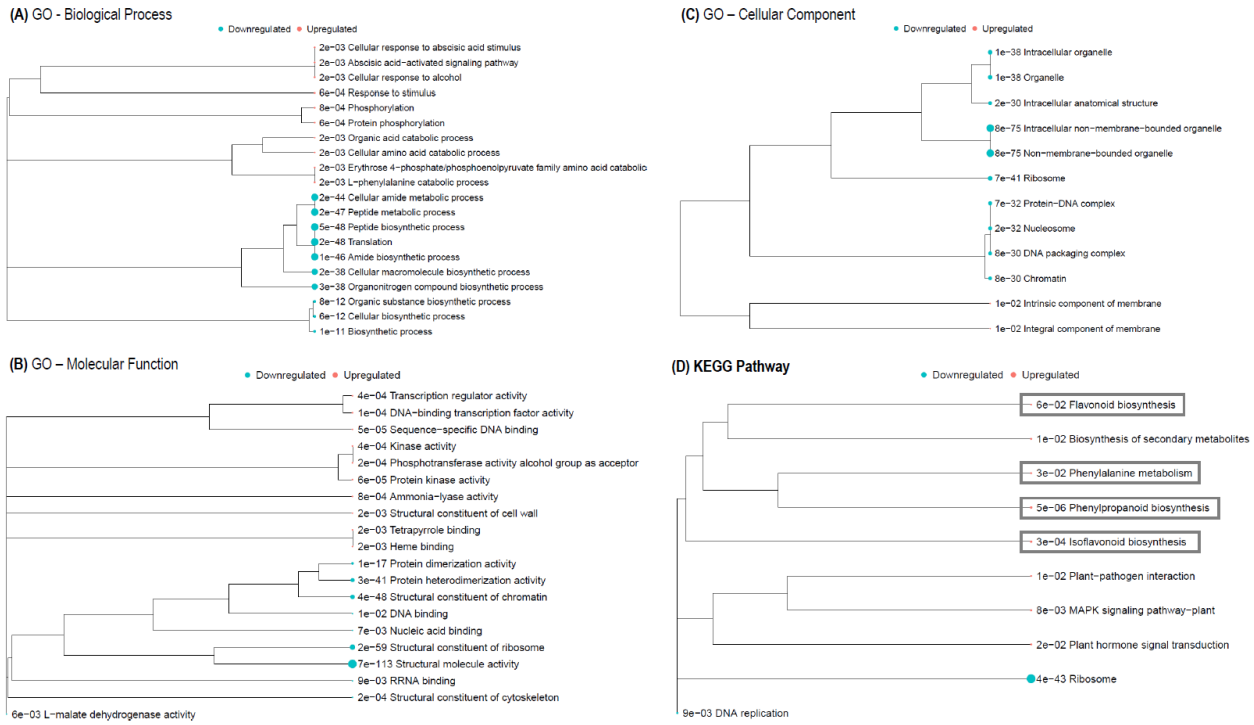

Fig. 4. Gene enrichment and functional analysis of differentially expressed genes (DEGs) in pea roots cultivated under Fe deficiency inoculated with T22: (A) biological process, (B) molecular function, (c) cellular component (d) KEGG pathway analysis.

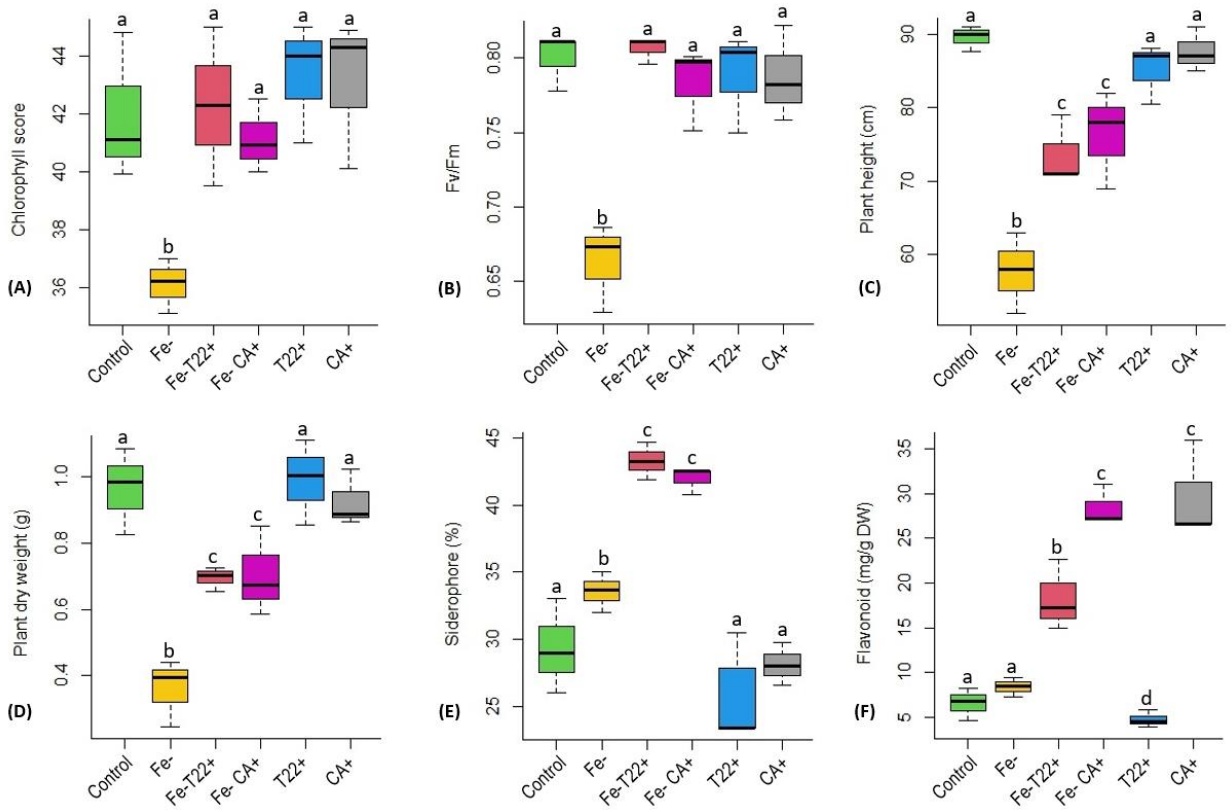

Fig. 5. Effect of cinnamic acid (CA) on chlorophyll score (A), Fv/Fm: maximal quantum yield of PS II (B), plant height (C), plant dry weight (D), rhizosphere siderophore (E) and root flavonoid content (F) in pea cultivated with or without the absence (control) or presence of Fe deficiency (Fe-) and T22. The data presented are means with standard deviations (n = 3 individual replicates). Statistically significant differences among the treatments at a $p < 0.05$ level were indicated by different alphabetical letters above the bars.

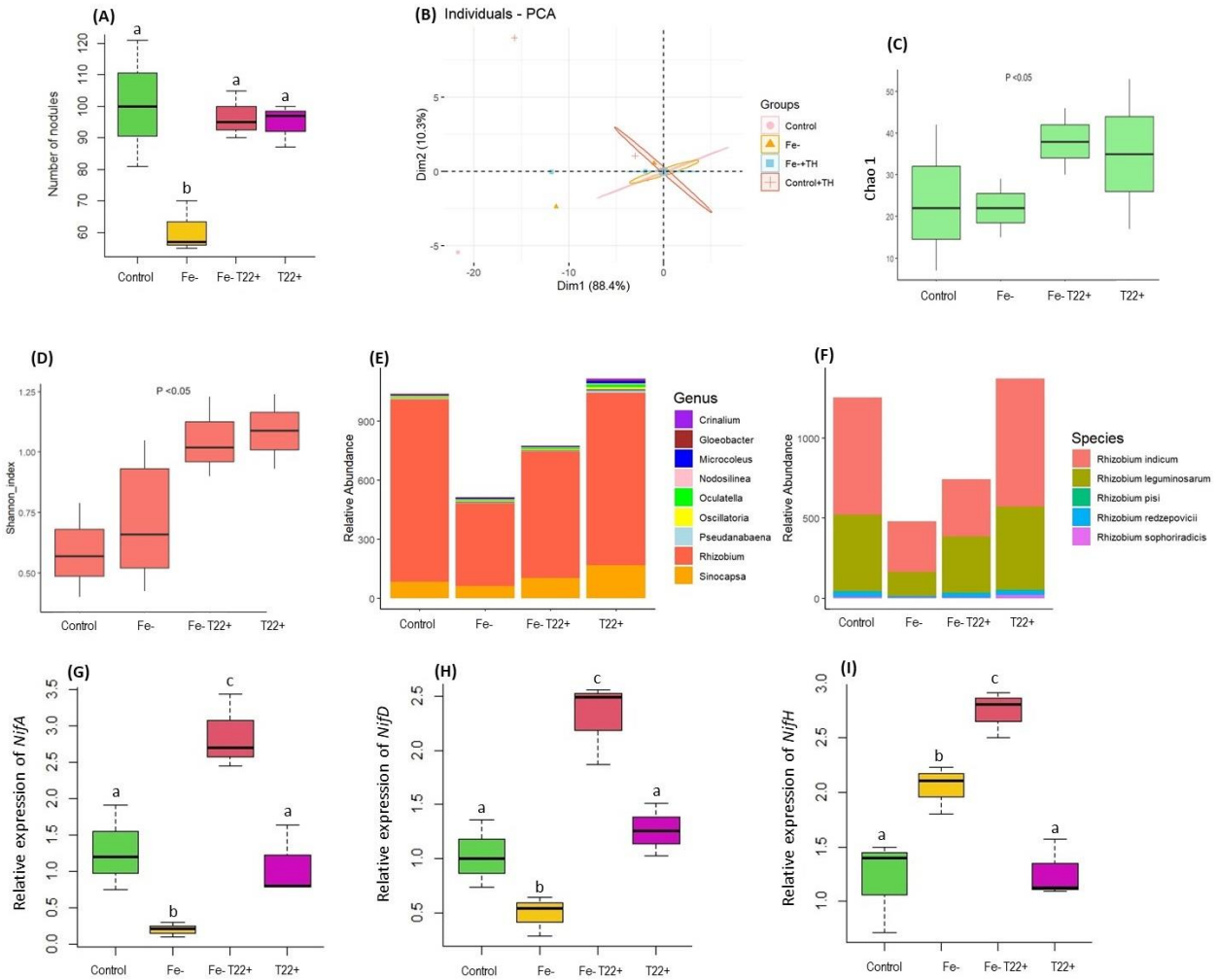

Fig. 6. Changes in nodule number (A), principal component analysis (B), Chao 1 (C), Shannon index (D), relative abundance of bacterial genera (E), relative abundance of *Rhizobium* species (F) as well as the expression of *NifA* (G), *NifD* (H) and *NifH* (I) in nodules of pea plants inoculated with or without T22 cultivated in the absence or presence of Fe deficiency. The data presented are means with standard deviations (n = 3 individual replicates). Statistically significant differences among the treatments at a $p < 0.05$ level were indicated by different alphabetical letters above the bars, where applicable.

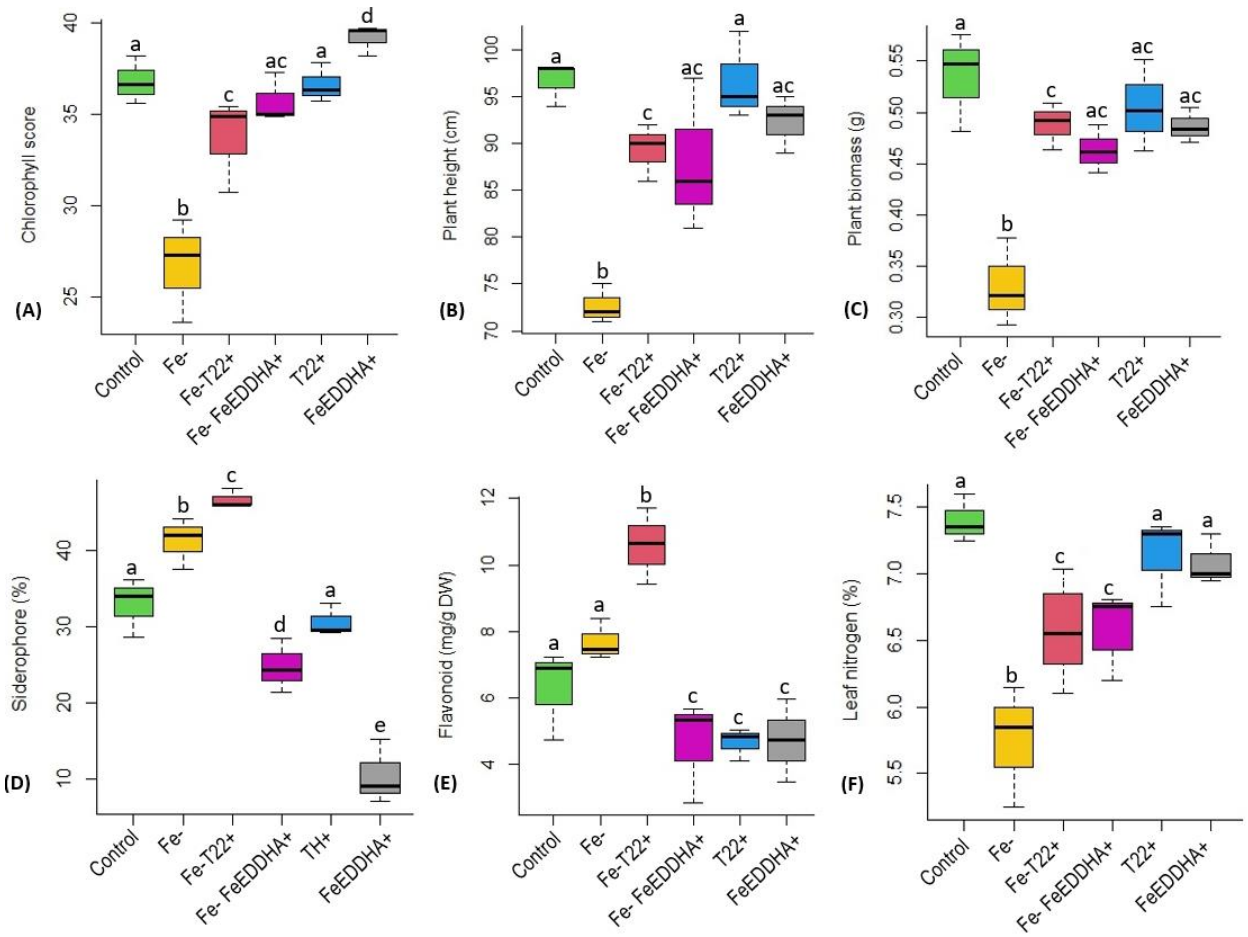

Fig. 7. Effect of FeEDDHA (Fe supplement) on chlorophyll score (A), plant height(B), plant biomass (C), rhizosphere siderophore (D), root flavonoid content (E) and leaf nitrogen (F) in pea plants cultivated with or without the absence (control) or presence of Fe deficiency (Fe-) and T22. The data presented are means with standard deviations (n = 3 individual replicates). Statistically significant differences among the treatments at a $p < 0.05$ level were indicated by different alphabetical letters above the bars.

.

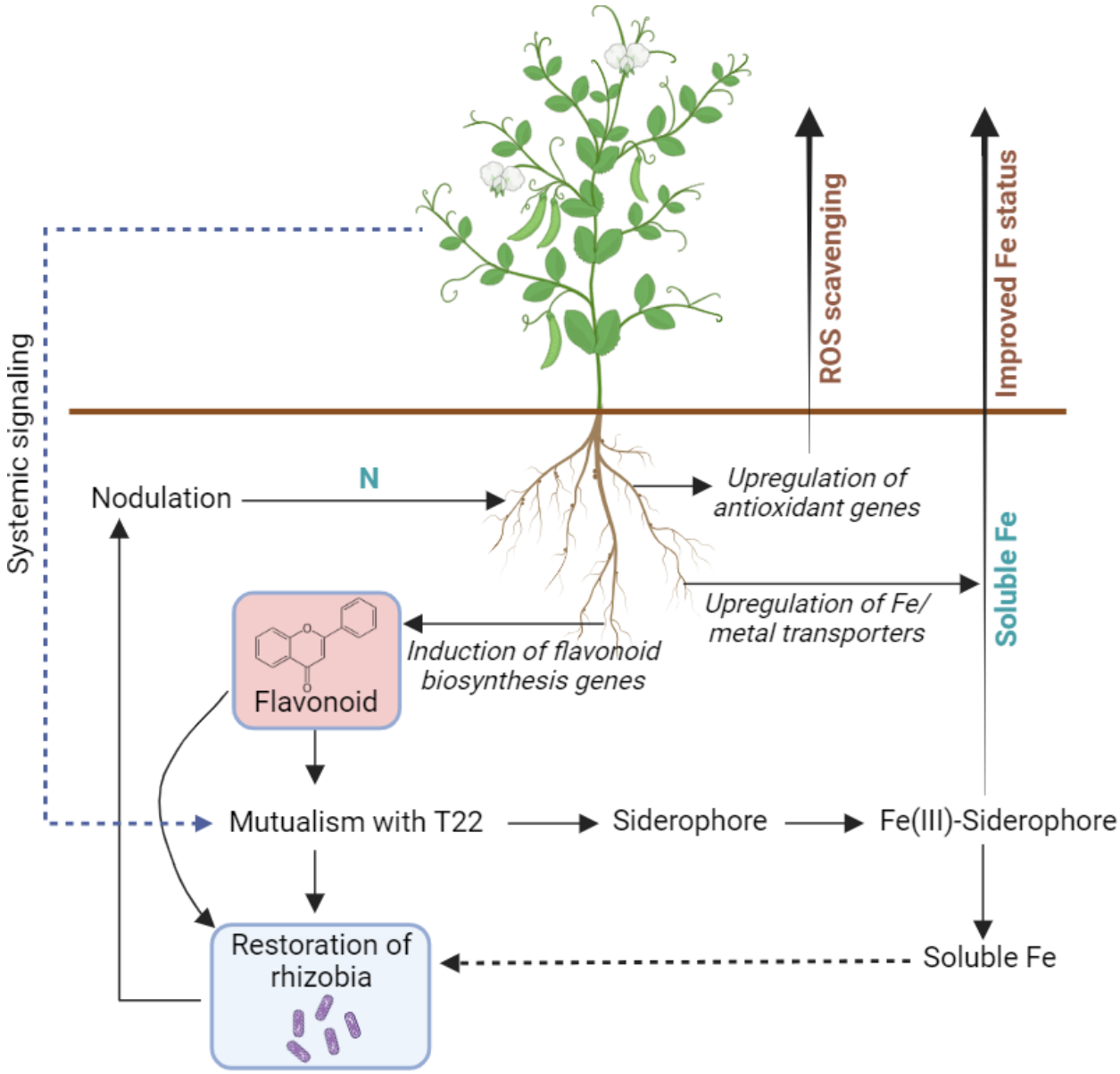

Fig. 8. Model of interactions by which T22 influences the symbiotic processes to help pea plants cope with Fe deficiency. Flavonoids, induced by specific biosynthesis genes in host plants, play a crucial role in mutualistic interactions with T22. This mutualism promotes the production of siderophores, which chelate Fe(III) and convert it into a soluble form that can be taken up by the induction of plant Fe/metal transporters. Additionally, the presence of T22 helps restore rhizobia populations through direct co-interaction or an Fe-mediated indirect pathway, facilitating N assimilation. T22 induces antioxidant genes in plants to regulate ROS status. Systemic signaling underlying symbiosis integrates these pathways, ensuring optimal plant health and growth in Fe-deficient soil.